Elsevier Editorial System(tm) for Powder Technology

Manuscript Draft

Manuscript Number: POWTEC-D-19-00339R1

Title: Fixed bed adsorption as affected by thermodynamics and kinetics: yellow tuff for CO2 capture

Article Type: Research Paper

Keywords: Fixed bed adsorption; Thermodynamics/Kinetics; Tuff; Zeolites; Langmuir/Freundlich isotherms; Pseudo-first/pseudo-second order kinetic models.

Corresponding Author: Dr. Federica Raganati, PhD

Corresponding Author's Institution: Istituto di Ricerche sulla Combustione IRC - CNR

First Author: Paola Ammendola, PhD

Order of Authors: Paola Ammendola, PhD; Federica Raganati, PhD; Riccardo Chirone, PhD; Francesco Miccio, PhD

Abstract: In this work, a yellow tuff has been proposed for the first time as sorbent for CO2 capture. Dynamic breakthrough experiments have been performed in a fixed bed reactor at different temperatures (25 - 150 °C) and CO2 partial pressures (0.01 - 0.20 atm), focusing on the process thermodynamics and kinetics. The thermodynamic and kinetic studies highlighted that the CO2 adsorption on the tuff in the low pressure region typical of combustion flue gases can be properly described by Freundlich's isotherm model and by the pseudo-first order kinetic model, respectively, thus indicating a physical, multilayer and heterogeneous surface binding mechanism. Based on the results obtained, it has been demonstrated that, in the framework of a real application for post-combustion CO2 capture, the natural tuff, i.e. a low-cost natural sorbent, could be more conveniently employed in vacuum swing or mixed mode in order to minimize the energy penalty of the process.

*Graphical Abstract (for review)

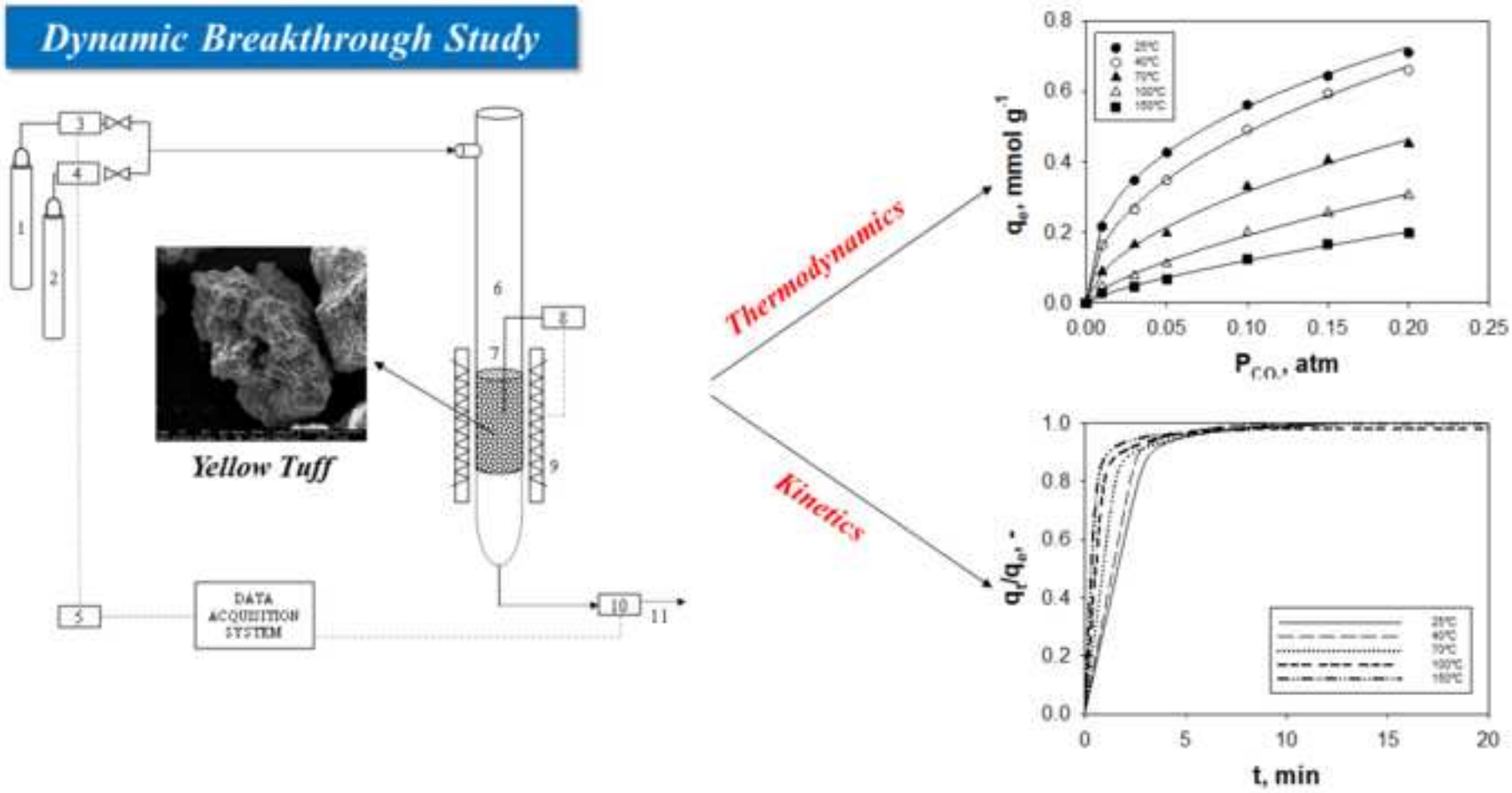

Highlights

1. CO_2 adsorption on a non-synthetic tuff zeolite was analyzed
2. Dynamic breakthrough experiments were performed in a lab-scale fixed bed reactor
3. Langmuir and Freundlich equations were used to model the CO_2 adsorption isotherms
4. CO_2 adsorption on the natural tuff is physical, multilayer and exothermic
5. The experimental data were finely fitted by a pseudo-first order kinetic model

Dear Editor,

enclosed please find both the rebuttal to the Reviewer's comments to the manuscript "Fixed bed adsorption as affected by thermodynamics and kinetics: yellow tuff for CO2 capture" and the revised version of the manuscript with changes marked-up using highlights.

The Authors thank the Reviewer for his/her comments on the paper and his/her helpful suggestions. In particular, besides some minor points, the Reviewers found that the original version of the manuscript suffers from some lack of information and discussion on some points that might lead to misunderstandings.

Then, following and accepting the Reviewer's comments and suggestions, the manuscript has been revised and, accordingly, improved.

See in the attached file the detailed answers (bold face) to the specific issues raised in the Reviewers' comments

Sincerely yours
Federica Raganati

ABSTRACT

In this work, a yellow tuff has been proposed for the first time as sorbent for CO_2 capture. Dynamic breakthrough experiments have been performed in a fixed bed reactor at different temperatures (25 – 150 °C) and CO_2 partial pressures (0.01 – 0.20 atm), focusing on the process thermodynamics and kinetics. The thermodynamic and kinetic studies highlighted that the CO_2 adsorption on the tuff in the low pressure region typical of combustion flue gases can be properly described by Freundlich's isotherm model and by the pseudo-first order kinetic model, respectively, thus indicating a physical, multilayer and heterogeneous surface binding mechanism. Based on the results obtained, it has been demonstrated that, in the framework of a real application for post-combustion CO_2 capture, the natural tuff, i.e. a low-cost natural sorbent, could be more conveniently employed in vacuum swing or mixed mode in order to minimize the energy penalty of the process.

Reviewer #2

We thank the Reviewer for his/her useful comments and precise suggestions. All the raised questions have been answered. See below a detailed answer to each comment.

1) Introduction could be shortened

Response to Reviewer's comment No. 1: Following the Reviewer's suggestion some parts of the introduction have been shortened in the revised version of the manuscript. Please, consider that new contents have been added, with respect to the original version of the manuscript, in order to answer some of the Reviewer's comments (see points n. 5 and 6).

2) It has been stated that the sorbent is subjected to a drying/cleaning step by flowing N2 at 150 °C. It has been later stated that the sorbent is pre-conditioned for about 10 min by setting the temperature (25, 40, 70, 100 and 150 °C) to the desired value. Is it possible to consider the drying step as a pre-condition step? Clarification is needed for the above statements.

Response to Reviewer's comment No. 2: We agree with the Reviewer on the necessity to better explain this part of the experimental procedure since, in its original version, it may be misleading. As also reported in the original version of the manuscript, the drying step, consisting in flowing N2 for 60min at 150 °C, is made in order to remove the water adsorbed on the tuff due to air humidity. After this drying step, the sorbent needs to be taken to the desired adsorption temperature. This is done during the step we called "pre-conditioning", i.e. the temperature is set to the desired value and N2 is continuously fluxed through the bed. Clearly, the actual duration of this "pre-conditioning" step depends on the adsorption temperature (25, 40, 70, 100 and 150 °C), i.e. it lasts until the sorbent reaches the set adsorption temperature starting from the drying temperature (150 °C).
Following the Reviewer's suggestion, the experimental procedure used prior to the adsorption step has been more clearly explained in the revised version of the manuscript.

3) Pre-condition time of the sorbent has been taken as 10 min. It would be good to indicate the basis for selection of 10 min.

Response to Reviewer's comment No. 3: Thanks to the Reviewer's comment n. 2, the pre-conditioning step has been more clearly explained in the revised version of the manuscript. In particular, the duration of this step depends on the set adsorption temperature (see point 2).

4) It has been stated on the Results and Discussion section about the adsorption temperature. Is it the temperature of the experiment? How many temperatures were employed? Clarification is needed for this aspect.

Response to Reviewer's comment No. 4: We thank the Reviewer for his/her comment. What we call "adsorption temperature" is the temperature set during the adsorption experiment. As also reported in the original version of the manuscript adsorption experiments have been performed at five different temperatures (25, 40, 70, 100 and 150 °C).
Following the Reviewer's comment, this aspect has been more clearly expressed in the revised version of the manuscript.

5) Breakthrough curves given in Fig. 2 provide useful information, such as time required to reach adsorption equilibrium. It is not clear whether this aspect has been taken into account.

Response to Reviewer's comment No. 5: We do agree with the Reviewer on the fact that the time needed to reach the adsorption equilibrium can be evaluated from the breakthrough curves (Fig. 3), i.e. the time at which the entire bed is in equilibrium with the feed (the outlet CO2 concentration is equal to the inlet CO2 concentration, C/C0=1). However, the time parameters typically evaluated from the breakthrough curves are the breakthrough time (tb) and Dt (t70-t10) rather than the equilibrium time [5,35,36]. The equilibrium time is not significant in the framework of a real CO2 adsorption process since the adsorption process would not be carried out until the complete saturation of the bed in order to achieve high separation efficiency. On the contrary, tb and Dt are indicative of the of the effective CO2 capture capacity of a sorbent and of the adsorption kinetics, respectively.
In a real industrial process, two fixed bed reactors would be used. The feed stream containing CO2 is passed through the first bed and, then, when breakthrough is about to occur, i.e. once the percentage of CO2 exiting the column rises above a certain threshold value (i.e. at the breakthrough value), the reactor is taken off-line and the feed is switched to the second bed. Simultaneously, the first bed is regenerated by either increasing the temperature (TSA) or decreasing the pressure (PSA), thus also recovering a high purity CO2 stream to be sent to the storage step. Therefore, the higher the breakthrough time is, the higher is the effective capture capacity (i.e. the higher is the fraction of bed used at breakthrough). Indeed, the reactor could be operated for longer time without regeneration, thus making the process more efficient from the economic point of view.
Likewise, while tb is indicative of the actual capture capacity of the sorbent, the time parameter Dt (t70-t10) can give a first indication on the adsorption kinetics [5,35,36], which the equilibrium time. Indeed, as also reported in the original version of the manuscript, Dt is related to the slope of the linear part of the breakthrough curve; the smaller this parameter is, the steeper the breakthrough curve and consequently the faster the adsorption kinetics will be. By the way, more detailed information on the adsorption kinetics are provided by the kinetic study (paragraph 5.4).
Following the reviewer comment, some of this consideration have been added to the revised version of the manuscript.

6) Authors claim that adsorption of CO2 on the adsorbent used is physisorption. If so, the interaction between the adsorbate and the adsorbent would not be strong, and desorption would take place effectively.

Response to Reviewer's comment No. 6: We do agree with the Reviewer's comment. Indeed, it has been proven that the CO2 adsorption capacity is strongly dependent on the structure and chemical surface of the adsorbent. Indeed, solid sorbents are conventionally classified on the basis of the typology of interaction that takes place between CO2 and the material: physical interaction (physisorption) and chemical interaction (chemisorption). In particular, physisorption arises from relatively weak interactions such as van der Waals force, while chemisorption involves stronger chemical interactions (chemical bonding) with consequent transfer of electrons between the adsorbent and adsorbate. In this framework, physical adsorption of CO2 is an attractive possibility because, the process is totally reversible, i.e. the sorbent can be easily and effectively regenerated with relatively small energy requirements due to the lower adsorption enthalpy in comparison to chemical sorbents.
Following the reviewer comment, some of this considerations have been added to the revised version of the manuscript.

7) Time taken to reach equilibrium with 20% (vol) exposure is much shorter as compared to 1% (vol) exposure. How would you explain this difference?

Response to Reviewer's comment No. 7: The fact that the time needed to saturate the bed (C/C0=1) increases with increasing the inlet CO2 concentration can be explained referring to the effect of the CO2 partial pressure (PCO2) on the adsorption process, as discussed in paragraph 5.2 also in the original version of the manuscript.
The results reported in Fig. 4 and table 2 show that an increase of PCO2 (i.e. an increase of the CO2 concentration in the feed stream) positively affects the adsorption kinetic. Indeed, Dt is decreased when PCO2 is increased, as also confirmed by the breakthrough curves becoming steeper (i.e. smaller times needed to saturate the bed). As a matter of fact, lower CO2 partial pressures result in slower breakthrough curves due to the CO2 concentration front taking more time to reach the outlet of the bed [5,32,56]. Also this result is in agreement with several works available in the literature on CO2 adsorption on physical sorbents [5,32,56].
Following the reviewer comment, this point has been more clearly explained in the revised version of the manuscript.

8) What would be attraction among CO2 molecules during multi-layer adsorption?

Response to Reviewer's comment No. 8: In the general adsorption isotherm theory the adsorption of molecules onto solid surfaces is classified as either monolayer or multilayer. In monolayer adsorption molecules are adsorbed in a one-molecule thick layer, i.e. all the adsorbed molecules are in contact with the sorbent surface. On the contrary, in multilayer adsorption the adsorption space accommodates more than one layer of molecules. In this framework, Langmuir's model is the simplest theoretical model to describe monolayer adsorption. However, often molecules do form multilayers, that is, some are adsorbed on already adsorbed molecules, and the Langmuir isotherm is not valid. On the contrary, Freundelich developed a model isotherm that takes that possibility into account. Typically, physical adsorption occurs through a multilayer mechanism, whereas, chemical adsorption occurs through a monolayer mechanism [46,49].
As regards the specific type of interaction between CO2 molecules, i.e. adsorbate-adsorbate interactions, they are typically van der Waals forces. In general, the van der Waals intermolecular forces comprise the Keesom (permanent–permanent dipoles) forces, Debye (permanent–induced dipoles) forces, and London dispersion (fluctuating dipole–induced dipole interaction) forces [75-77].
Then, it should be considered that CO2 is a non-polar molecule based on its structure. Indeed, in spite of the polar bonds between the central carbon and the two oxygen atoms, the dipoles cancel out because they act in opposite directions [75-77]. As a consequence, CO2 molecules cannot interact through permanent dipole-dipole interactions. Therefore, CO2 can only interact through London dispersion intermolecular forces caused by temporary instantaneous dipoles from random movements of electrons [75-77].
Following the reviewer comment, this point has been more clearly explained in the revised version of the manuscript.

9) Adsorption isosteres of CO2 on the natural tuff for different loadings lead to different slopes? Explanation is needed for this trend.

Response to Reviewer's comment No. 9: As also discussed in the original version of the manuscript, the slope of the adsorption isosteres is associated to the values of the isosteric heat of adsorption (Qst), defined as the heat of adsorption at constant amount of adsorbed CO2 (qe). In particular, Qst at a given loading qe can be calculated, after integrating the Clausius–Clapeyron equation, from the slopes of the adsorption isosteres (i.e. the plots of lnPCO2 against 1/T at a fixed specified adsorbed amount of CO2) [25,30,52] (see paragraph 3.2).

Then the fact that the adsorption isosteres have different slopes depending on the surface loading (qe) means that Qst depends on the surface loading. As also stated in the orginal version of the manuscript, the dependence of Qst on the surface coverage can be used as criteria for determining the energetic heterogeneity of a solid surface. Indeed, Qst is independent of the surface coverage when no interaction occurs between adsorbed molecules and the surface is energetically homogeneous [45,51,52]. On the contrary, a variation of Qst with the surface loading indicates the existence of different levels of surface energy and heterogeneity of the adsorbent surface [45,51,52].
More specifically, for the tested tuff, it has been found that the Qst (Fig.9), i.e. the slope of the adsorption isosteres (Fig. 8), decreases with increasing CO2 surface loading, which means that the tuff is characterized by a high level of heterogeneity and that there is a variation in adsorbate-adsorbent and adsorbate-adsorbate interactions [79]. In general, Qst is associated with the interaction between CO2 molecules and the adsorbent surface through different kinds of adsorptive molecular forces, such as Van der Waals forces, hydrophobicity, ligand exchange and chemical bond [80]. At the initial stages of adsorption, large numbers of free adsorption sites are available on the tuff surface. As a consequence, the CO2 molecules may easily come into direct contact with adsorbent surface, more intense forces being present between CO2 molecules and the adsorbent; as a consequence, the activation energy is low and the heat of adsorption is high. As the adsorption process continues to take place, i.e. the surface coverage is increased, less and less adsorption sites are still available and, as a consequence, the adsorption of further CO2 molecules becomes more and more difficult. Besides that, with the surface coverage increasing, also adsorbate-adsorbate interactions start to occur. Therefore, it is most likely that some kind of lateral interactions in the adsorbed layers take place in the form of attractive/repulsive London dispersion intermolecular forces between adsorbed CO2 [79,81,82]. As a result, as the adsorption process proceeds, the activation energy is increased and the heat of adsorption is decreased [83,84].
Following the Reviewer's comment this point has been more clearly explained in the revised version of the manuscript.

10) Clear explanation is needed on why CO2 is adsorbed in a much larger amount than CH4.

Response to Reviewer's comment No. 10: The fact that CO2 is adsorbed on the tuff in a much larger amount than CH4 can be explained referring to the crystalline structure of the material (i.e. dimension of pore openings) and to the kinetic diameters of CO2 and CH4.
As a consequence of their crystalline structure, zeolites have narrow pore openings and a uniform pore size distribution and thus show great potential for the separation of small gas molecules. Synthetic zeolites such as 13X and 5A are among the most commonly used adsorbents in industrial gas separations [73-76], but several naturally occurring zeolites including clinoptilolite, mordenite, and chabazite have pore structures and chemistry that may also be suitable for the separation of CO2 from CH4 [73-76]. In particular, the tested tuff has been found to be characterized by a rather high level of cristallinity, with characteristic reflection peaks of chabazite, as also reported in the original version of the manuscript (paragraph 5.1).
Chabazite (structural formula (Ca2,Na4,K4)[(AlO2)4(SiO2)8] 13H2O) has a three-dimensional framework delimited by eight-membered rings that create pore openings of 0.38 nm, i.e. very close to the kinetic dimension of CH4 (0.38 nm). Then, considering that the kinetic dimension of CO2 (0.33 nm) is remarkably smaller than CH4, chabazite and chabazite-like zeolites (and also other 8 rings zeolites) can be used as selective adsorbents for CO2 from natural gas. As a matter of fact, they can allow for a kinetically enhanced CO2-over-CH4 selectivity [73-76].

Following the Reviewer's suggestion some of these considerations have been added to the revised version of the manuscript.

11) According to Fig. 3, time taken to reach adsorption equilibrium depends on experimental conditions. For certain loadings, it is very fast. It is not certain whether this aspect was considered in designing kinetics experiments because such experiments should be performed before the equilibrium is established. On the other hand, when applying pseudo order conditions, concentration of one of the reactants should be maintained at a higher value so that its concentration would not be significantly changed during the cause of the reaction. Otherwise pseudo order conditions cannot be applied. It is not certain whether this issue has been taken into consideration. Clarifications are needed for the above issues.

Response to Reviewer's comment No. 11: We thank the Reviewer for his/her comment, however we think that there have been some misunderstandings regarding the kinetic study. We will try to explain it in a clearer way.
As regards the point that "time taken to reach adsorption equilibrium depends on experimental conditions", we totally agree with the Reviewer. Indeed, as also discussed in points 3 and 7, adsorption is fastened, i.e. the time needed to reach the equilibrium decreases, by increasing temperature and CO2 partial pressure (as clearly shown in Fig. 3 by the breakthrough curves becoming steeper). This has been actually considered in the designing of the adsorption experiments, since, as correctly highlighted by the Reviewer, kinetic analysis has to be performed before adsorption equilibrium.
We do understand that the use of the term "pseudo" may lead to possible misunderstanding. Indeed, as correctly highlighted by the Reviewer, the prefix "pseudo", when applied to chemical kinetics, refers to systems in which one of the reactants is held sufficiently constant during the reaction so that it does not need to be included in the mathematical expression of the reaction rate [57-60]. However, in the framework of the adsorption study, the word "pseudo" is used to imply that a rate law for adsorption is expressed in terms of an adsorbed amount (q) (i.e. occupied sites of adsorption) rather than in terms of concentration of the adsorbing species [57-60].
In this framework, Lagergren's first-order rate equation is the earliest known one describing the adsorption rate based on the adsorption capacity. It is a first-order kinetic model since it assumes that the rate of adsorption is proportional to the number of available free active sites on the adsorbent surface. Itss mathematical expression is given by [55]:

(Equation 6)

Where kf is the first-order kinetic constant (1/min), qe and qt (mg/g) are the adsorption capacities at equilibrium and at time t (min), respectively,.
With the boundary conditions of t =0, qt = 0 and t = inf, qt = qe, it can be expressed as:

(Equation 7)

Likewise, the second-order rate equation was firstly introduced by Blanchard et al. [56] and it is based on the assumption that the adsorption rate is proportional to the square of the number of vacant adsorption sites. Its mathematical expression is given by:

(Equation 8)

where, ks (min-1) is the second order kinetic constant. With the boundary conditions of t =0, qt = 0 and t = inf, qt = qe, it can be expressed as:

(Equation 9)

Then, the prefix "pseudo" was added and the adsorbed amount-based first-order and second-order rate equations by Lagergren [55] and Blanchard et al. [56], respectively, were called pseudo-first and pseudo-second order models just in order to distinguish them from kinetic equations based on concentration.
Following the Reviewer's comment some of these considerations have been added to the revised version of the manuscript for the sake of clarity.

12) Authors should comment on limitations associated with applying theories of equilibrium and kinetics, which are typically applied for stationary systems, on dynamic systems where a flow of CO2 is used in experiments.

Response to Reviewer's comment No. 12: We thank the Reviewer for his/her comment, however, the methodological approach used in this work to study adsorption thermodynamics and kinetics is widely accepted and used in the specialized literature in the case of both stationary and dynamic (i.e. adsorption studies performed though breakthrough experiments) systems.
As regards, the thermodynamic study, all the evaluation have been made on the basis of data obtained once the thermodynamic equilibrium has been reached, regardless of the dynamic nature of the breakthrough experiments. In particular, according to the specialized literature, the equilibrium of adsorption has been described by adsorption isotherms, i.e. a graphical representation showing the relationship between the amount adsorbed by a unit weight of adsorbent and the amount of adsorbate present in the gaseous medium (i.e. the CO2 partial pressure) at equilibrium (i.e. C/C0 =1) and at a fixed temperature. In other words, it maps the distribution of adsorbable CO2 between the gaseous and solid phases at various equilibrium concentrations (i.e. PCO2). More specifically, when the adsorption study is performed through breakthrough experiments (typically in fixed bed reactors), which are intrinsically dynamic, the points of the CO2 adsorption isotherms, i.e. the specific equilibrium amounts of adsorbed CO2 for a specific temperature and CO2 partial pressure, are determined by integrating the breakthrough curves according to the mass balance equation (Eq. 1) applied to the system (as also reported in the original version of the manuscript).
As regards the kinetic study, considering that the prediction of kinetic parameters of the adsorption process is typically complex, the most used and widely accepted approach consists in fitting the experimental data to different available apparent kinetic models and, then, select the one characterized by the best fitting [51-54]. The main characteristic of these apparent models is that all the adsorption steps, i.e. all the mass transfer resistances, such as external diffusion, pore diffusion, and surface adhesion, are lumped together [51-54]. Among all the available kinetic models, two of the most commonly applied, also in the framework of CO2 adsorption studies [51-54], are the pseudo-first and pseudo-second order kinetic models.
Following the Reviewer's comment some of these considerations have been added to the revised version of the manuscript for the sake of clarity.

Fixed bed adsorption as affected by thermodynamics and kinetics: yellow tuff for CO_2 capture

Paola Ammendola[1], *Federica Raganati*[1,*], *Riccardo Chirone*[1], *Francesco Miccio*[2]

[1]Istituto di Ricerche sulla Combustione (IRC) - CNR, Piazzale V. Tecchio 80 - 80125 Naples, Italy

[2]Istituto di Scienza e Tecnologia dei Materiali Ceramici (ISTEC) - CNR, via Granarolo, 64 - 48018 Faenza (RA), Italy

[*]Corresponding author

Tel.:+39 0817682237; fax:+39 0815936936.

E-mail address: federica.raganati@irc.cnr.it

ABSTRACT

In this work, a yellow tuff has been proposed for the first time as sorbent for CO_2 capture. Dynamic breakthrough experiments have been performed in a fixed bed reactor at different temperatures (25 – 150 °C) and CO_2 partial pressures (0.01 – 0.20 atm), focusing on the process thermodynamics and kinetics. The thermodynamic and kinetic studies highlighted that the CO_2 adsorption on the tuff in the low pressure region typical of combustion flue gases can be properly described by Freundlich's isotherm model and by the pseudo-first order kinetic model, respectively, thus indicating a physical, multilayer and heterogeneous surface binding mechanism. Based on the results obtained, it has been demonstrated that, in the framework of a real application for post-combustion CO_2 capture, the natural tuff, i.e. a low-cost natural sorbent, could be more conveniently employed in vacuum swing or mixed mode in order to minimize the energy penalty of the process.

Keywords: Fixed bed adsorption; Thermodynamics/Kinetics; Tuff; Zeolites; Langmuir/Freundlich isotherms; Pseudo-first/pseudo-second order kinetic models.

1. Introduction

Among all the CO_2 separation strategies, i.e. post-combustion capture, pre-combustion capture and oxy-fuel combustion [1], developed in the framework of Carbon Capture and Storage (CCS) [2], post-combustion capture, which consists in the selective removal of CO_2 from the gaseous effluent, represents a near-term solution for stationary fossil fuel-fired plants, since it does not need any radical change to existing facilities and processes [3]. Even though being the most mature thechnology for CO_2 separation [4], amine-based or ammonia-based absorption methods suffer from severe drawbacks when applied to post-combustion applications: high energy requirement for sorbent regeneration, corrosion issues, thermal/chemical degradation of the amines due to the presence of oxygen and amine losses due to evaporation, causing environmental impact [4]. In this framework, adsorption using solid sorbents has attracted great interest since it is characterized by low regeneration energy consumption, high selectivity, easiness in handling, no liquid waste streams and applicability over a relatively wide range of operating temperatures [5]. Adsorption is typically carried out in two fixed bed reactors. The feed stream containing adsorbate is passed through the first bed and, then, when breakthrough is about to occur, i.e. once the percentage of the adsorbate exiting the column rises above a certain threshold value (i.e. at the breakthrough value), the reactor is taken off-line and the feed is switched to the second bed. Simultaneously, the first bed is regenerated by either increasing the temperature (temperature swing adsorption, TSA) or decreasing the pressure (pressure swing adsorption, PSA). However, for the success of this approach the sorbent should combine low cost with versatility and good performances at low CO_2 pressure (up to 0.2 atm in typical post-combustion conditions [3]) in terms of a high CO_2 adsorption capacity, fast adsorption/desorption kinetics, high CO_2 selectivity, mild regeneration conditions, high stability to cyclic adsorption–desorption operations, tolerance to the presence of moisture and other impurities in the feed and adequate mechanical strength [5]. In this context, sorbents are classified as either physical or chemical sorbents [6]. In particular, physisorption arises from

relatively weak interactions such as van der Waals force, while chemisorption involves stronger chemical interactions (chemical bonding) with consequent transfer of electrons between the adsorbent and adsorbate [6]. Common materials acting as physisorbent are porous carbonaceous materials [5,7–12], zeolites [13,14], alumina [15], silica gels [16] and geopolymers [17,18]. On the contrary, chemical sorbents, such as amine-functionalized sorbents, have basic sites (carbonates and amino groups) capable of strongly interact with the acidic CO_2 molecules [19,20]. Other sorbents, such as metal organic frameworks (MOFs), are capable of providing both physical and chemical interactions with CO_2 [21,22]. In this framework, physical adsorption of CO_2 is an attractive possibility because, the process is totally reversible, i.e. the sorbent can be easily and effectively regenerated with relatively small energy requirements due to the lower adsorption enthalpy in comparison to chemical sorbents [3]. Synthetic zeolites are highly ordered microporous crystalline materials, synthetized with a very precise and suitable molecular cell, pore size and nature of extra-framework cations, thus specifically affecting their adsorption performance [23]. However, their high synthesis cost and the environmental footprint represent a negative contribute to their sustainability [17,24]. A possible alternative is provided by natural occurring zeolites, as they are available in large quantities in different regions of the world in the natural composition of different types of rocks [25,26]. Their abundance and low or null price, somehow, offset some unavoidable drawbacks such as variable composition that may change even in a single deposit, low purity and likely poorer separation performance compared to the more-performant synthetic zeolites [25]. In this framework, the volcanic tuffs are the most valuable deposits of natural zeolites [27] and they are characterized by the presence of different minerals, such as: clinoptilite, mordenite, chabazite, quartz, cristobalite, feldspar, etc. [28]. Natural zeolites were promisingly tested for biogas purification [29,30]. Nonetheless, the literature about the use of natural tuff as CO_2 adsorbent at low pressure is still lacking.

After the selection of the adsorbent material, a combined study of the equilibrium and kinetics is necessary for the design of the specific adsorption system (such as pressure swing and temperature swing). Indeed, the accurate mathematical representation of both the adsorption equilibrium and kinetics is crucial for the identification of the adsorption performances, by providing useful insight into the adsorbate-adsorbent interactions [31,32]. In particular, a good adsorbent should provide the right compromise between high equilibrium adsorption capacity and fast kinetics [31,32] that are requisites for process implementation.

This work is aimed at investigating the low-pressure CO_2 adsorption on a natural zeolite tuff, with particular attention to its mechanism, in terms of thermodynamics and kinetics. Dynamic breakthrough tests have been carried out in a lab-scale fixed bed reactor at different adsorption temperatures (25 - 150 °C) and CO_2 partial pressures (1 - 20 %vol.). Langmuir and Freundlich isotherm models have been used to fit the equilibrium experimental equilibrium data, thus providing insights into the feasibility and strength of adsorbate–adsorbent interaction. Pseudo-first and pseudo-second order kinetic models have been used to fit the experimental CO_2 uptake data, thus obtaining the rate of CO_2 adsorption for possible equipment design. The unpublished results of CO_2 adsorption by means of natural tuff are reported and discussed in the article, along with theoretical speculations for practical use in post-combustion CO_2 removal.

2. Experimental

2.1 Materials

A natural yellow tuff from Campania (I) region has been used as adsorbent material. The sample has been crushed and sieved to obtain a 400-600 μm fraction. The main physical properties of the yellow tuff are reported in Table 1. Prior to the CO_2 adsorption study, the tuff physical and structural properties have been characterized. The internal porosity and the absolute density of the material have determined by employing mercury intrusion porosimetry (MIP, ThermoFinnigan

240). XRD analysis has provided the phase composition of the tuff by using a Bruker D8 Advance powder diffractometer with Cu Kα radiation. In particular, the sample has been analyzed after drying at 100 °C and heating up to 250 °C in order to check possible changes of the phases in the material due to the thermal treatment. The results are discussed in section 5.1. The specific heat, determined with calorimetric procedure at room temperature, is in the typical range of lapideous materials. Also the minimum fluidization velocity of the tuff has been theoretically evaluated [33].

2.2 Experimental apparatus and procedure for CO_2 adsorption tests

The CO_2 dynamic adsorption breakthrough tests were carried out at atmospheric pressure and at different temperatures (25, 40, 70, 100 and 150 °C) in a laboratory-scale fixed bed reactor (ID = 10 mm, column length = 600 mm) reported in Figure 1.

A type K thermocouple, with a diameter of 1 mm, connected to a PID controller is used to monitor the temperature and keep it at the desired value, by means of an electric heating jacket (Tyco Thermal Controls GmbH).

Separate high purity N_2 and CO_2 cylinders (99.995% vol.) are used to prepare the gas feed, using two mass flow controllers (Brooks 8550S) to set and control the inlet flowrates. The analysis system consists of a continuous gas analyzer equipped with an infrared detector (ABB AO2020, URAS 14), monitoring the outlet CO_2 concentration during the transient adsorption process.

In a typical adsorption test, the sorbent (5 g, corresponding to about 5 cm of bed height) is subjected to a drying/cleaning step by flowing N_2 (15 L h^{-1}) for 60 min at 150 °C and atmospheric pressure. This step is necessary since zeolites are very sensitive to the presence of water, which strongly inhibits their CO_2 adsorption performances [25]. Afterwards, during a pre-conditioning step, the temperature is set to the desired adsorption temperature (25, 40, 70, 100 and 150 °C) and N_2 is continuously fluxed through the bed (15 L h^{-1}). Clearly, the actual duration of this pre-conditioning step depends on the adsorption temperature, i.e. it lasts until the sorbent reaches the set adsorption temperature starting from the drying temperature (150 °C). Then, once the desired

adsorption temperature is reached, the adsorption is started, in which 15 L h^{-1} of the CO_2/N_2 gas mixture (1, 3, 5, 10, 15 and 20 % vol. of CO_2) is fed through column. By continuously monitoring the CO_2 concentration in the outlet stream until saturation of the bed (i.e. the outlet CO_2 concentration approached the inlet value) the breakthrough curves are obtained.

Adsorption tests have been also carried out to measure the selectivity of the tuff for CO_2 over CH_4. The CH_4 adsorption isotherm has been obtained at ambient temperature by using the same operating conditions as those of the CO_2 adsorption tests (CH_4/N_2 mixture inlet flow rate of 15 L h^{-1}; 1, 3, 5, 10, 15 and 20 % vol. of CH_4); the outlet CH_4 concentration has been monitored using the same analysis system as that used for the CO_2 adsorption tests. Then, the CO_2/CH_4 selectivity factor has been estimated based on the measurement of pure fluids equilibrium capacities. In particular, it is the ratio between the equilibrium molar uptakes of CO_2 and CH_4 at a given pressure taken from the corresponding single component isotherms [34].

For each CO_2 adsorption test the breakthrough curve has been obtained, i.e. a plot reporting C/C_0 versus time, being C and C_0 the volumetric CO_2 concentration in the outlet and inlet stream, respectively. By subsequent elaboration of the data the most important adsorption parameters have been calculated [5,35,36]:

i) the amount of CO_2 adsorbed per unit mass of adsorbent, q_e, obtained from the integration of the breakthrough curves in accordance to a mass balance equation applied to the adsorption column

$$q_e = \frac{1}{m}\int_0^{t_s}\left(F_{CO_{2,in}} - F_{CO_{2,out}}\right)dt \quad (1)$$

where m is the mass of sorbent in the bed, $F_{CO2,in}$ and $F_{CO2,out}$ are to the molar flowrate of CO_2 at the inlet and outlet of the bed, respectively, t_s is to the time needed to saturate the bed of sorbent;

ii) the breakthrough time, t_b, i.e. the time in which the CO_2 concentration at the outlet of the column is the 5% of the inlet concentration; it is the time at which the reactor is taken off-line for regeneration, i.e. the higher t_b is the higher the effective capture capacity is;

iii) the time parameter $\Delta\tau = t_{70} - t_{10}$ (with t_{10} and t_{70} being the time for which CO_2 reach 70% and 10% of the inlet concentration at the adsorption column outlet) that is tightly linked to the slope of the linear part of the sigmoid (the smaller $\Delta\tau$ is, the steeper the breakthrough curve and consequently the faster the adsorption will be);

iv) the fraction of bed used at breakpoint ψ, i.e. the percentage of CO_2 adsorbed until t_b with respect to the total amount adsorbed upon saturation.

3. Adsorption thermodynamics

3.1 Adsorption isotherms

The adsorption equilibrium is typically described by adsorption isotherms, i.e. graphical representation of the relationship between the equilibrium CO_2 uptake (i.e. the amount of CO_2 adsorbed at equilibrium by a unit weight of the sorbent) and the CO_2 partial pressure at equilibrium and at fixed temperature. The equilibrium CO_2 uptake for a certain temperature and CO_2 partial pressure is computed by integrating the breakthrough curves [31]. In particular, among all the available isotherms models, Langmuir and Freundlich models have been employed to fit the experimental adsorption isotherms of the tuff, according with most of the works available on CO_2 adsorption on physical sorbents (such as activated carbons and zeolites) [37–45]. A non-linear regression analysis has been used because of the issues associated with the linearization of non-linear isotherm equations [46].

The Langmuir model [47] is the simplest theoretical model to describe monolayer adsorption onto homogeneous surfaces (i.e. the adsorption sites are equivalent from an energetic point of view) and it is based on the following mathematical expression [47]:

$$q_e = q_L \frac{K_L P_{CO_2}}{1+K_L P_{CO_2}} \quad (2)$$

where q_e (mmol g^{-1}) is the amount of CO_2 adsorbed per mass of sorbent at equilibrium, q_L (mmol g^{-1}) is the maximum monolayer adsorption capacity of the adsorbent, P_{CO2} (atm) is the equilibrium pressure of the gas adsorbed, whilst K_L (atm^{-1}) is the Langmuir adsorption constant or affinity constant (larger values of K_L indicating a stronger adsorbate/adsorbent affinity with a wider surface coverage). Another important parameter is the dimensionless separation factor or equilibrium parameter, R_L, defined as:

$$R_L = \frac{1}{1+K_L P_{CO_2}} \quad (3)$$

The value of R_L indicates the shape of the isotherm ($R_L > 1$ unfavorable; $R_L = 1$ linear; $R_L = 0$ irreversible; $0 < R_L < 1$ favorable) [47].

Adsorption of molecules on surfaces having constant energy of interaction is very rare in practice, i.e. most solids are very heterogeneous in contrast to the hypothesis made by Langmuir. Therefore, the likely heterogeneity of the sorbent surface is taken into account by assuming that the interaction energy follows some kind of mathematical distribution. One of the most used isotherm models to take into account this (also in the case of CO_2 adsorption) [37–45] is the Freundlich model [48], providing the first empirical equation to describe non-ideal multilayer adsorption (i.e. several layers of adsorbate can be attached on the adsorbent) onto heterogeneous surfaces [46,49]. The main assumption is that the adsorption energy exponentially decreases as the number of available adsorption sites decreases (i.e. with increasing surface coverage) [48], in contrast to the Langmuir model. Its mathematical expression is:[48]

$$q_e = K_F {P_{CO_2}}^{1/n} \quad (4)$$

where K_F is the Freundlich isotherm constant (mmol g^{-1} $atm^{-1/n}$) and n is the heterogeneity factor (Freundlich coefficient). The ratio 1/n is the Freundlich intensity parameter and it is a measure of the adsorbate/adsorbent binding energy and surface heterogeneity [48]. Moreover, the magnitude of

1/n gives insight on whether the process is favorable or not, the adsorption being favorable at 1/n < 1 [48].

The quality of the isotherm fit by Lamgmuir and Frenundlich models to experimental data has been assessed by evaluating the coefficient of correlation, R^2, changing between 0 to 1, and the HYBRID error function, proposed for improving the fit of the sum of the squares of errors (SSE) method at low partial pressure values [39], where the lower the HYBRID value the better the fitting quality is. In particular, it is defined as:

$$HYBRID(\%) = \frac{100}{n-p}\sum_{i=1}^{i=n}\left[\frac{\left(q_{mod_i}-q_{exp_i}\right)^2}{q_{exp_i}}\right] \quad (5)$$

where q_{exp} and q_{mod} are the experimental and modeled adsorption uptakes, respectively, n is the number of experimental points and p is the number of parameters of the equation.

3.2 Evaluation of thermodynamic properties

The most important thermodynamic parameters, i.e. the standard Gibbs free energy change (ΔG^0, kJ mol^{-1}), the enthalpy change (ΔH^0, kJ mol^{-1}), and the entropy change (ΔS^0, kJ mol^{-1}) have been evaluated combining the thermodynamic laws with the experimental data obtained from the Langmuir isotherms and by applying the van't Hoff equation [26,50]. The analysis of these parameters can give information on nature the adsorbent-adsorbate interactions [50]. The adsorption process is spontaneous if the total free energy of the system decreases ($\Delta G^0 < 0$). The process is either exothermic or endothermic if $\Delta H^0 < 0$ and > 0, respectively [50]. Moreover, for physical adsorption $|\Delta H^0| < 20$ kJ mol^{-1}, whereas for chemisorption $|\Delta H^0| > 40$ kJ mol^{-1} [50]. The organization of the adsorbate at the solid/gaseous interface during the adsorption process becomes less random if $\Delta S^0 < 0$ or more random if $\Delta S^0 > 0$.

Another key parameter is the isosteric heat of adsorption (Q_{st}) [51], defined as the heat of adsorption at constant amount of adsorbed adsorbate. It can provide an estimation of the strength of molecular-scale interactions between the adsorbate molecules and the adsorbent surface, $Q_{st} < 80$ kJ

mol^{-1} applying for physisorption and Q_{st} = 90-100 kJ mol^{-1} for strong chemisorption [46,52,53]. Moreover, information regarding its magnitude and dependence on the surface coverage can be used as criteria for determining the energetic heterogeneity of a solid surface [46,52,53]. Indeed, Q_{st} is independent of the surface coverage when no interaction occurs between adsorbed molecules, and the surface is energetically homogeneous [46,52,53]. On the contrary, a variation of Q_{st} with the surface loading indicates the existence of different levels of surface energy and heterogeneity of the adsorbent surface [46,52,53]. Q_{st} at a given q_e can be calculated, after integrating the Clausius–Clapeyron equation, from the slopes of the plot of $\ln P_{CO2}$ against 1/T at a fixed specified adsorbed amount of CO_2 (i.e. slopes of adsorption isosteres) [26,31,53].

4. Adsorption kinetics

Since the prediction of kinetic parameters of the adsorption process is typically complex, the most used approach consists in fitting the experimental data to different available apparent kinetic models and, then, select the one characterized by the best fitting [54–57]. Among the kinetic models available in the literature, pseudo-first order [58] and pseudo-second order [59] models are the simplest and most extensively used ones [54–57]. It is noteworthy to underline that, when used in the framework of adsorption kinetic studies, the prefix “pseudo” does not have its most classic connotation deriving from chemical kinetics (i.e. referring to systems in which one of the reactants is held sufficiently constant during the reaction so that it does not need to be included in the mathematical expression of the reaction rate) [60–63]. Indeed, it is used just to imply those rate laws for adsorption expressed in terms of adsorbed amounts (q) (i.e. occupied sites of adsorption) rather than in terms of concentration of the adsorbing species [60–63]. The main characteristic of these apparent models is that all the adsorption steps, including mass transfer resistances, such as external diffusion, pore diffusion, and surface adhesion, are grouped together [54–57]. Besides that, it is also assumed that the difference between the equilibrium concentration and the average solid phase concentration is the driving force for adsorption.

The pseudo-first order kinetic model was first introduced by Lagergren in 1898 [58]. The main assumption of the pseudo-first order kinetic model is that the rate of adsorption is proportional to the number of available free active sites on the adsorbent surface. Its rate expression in the differential form is expressed as [58]:

$$\frac{dq_t}{dt} = k_f(q_e - q_t) \quad (6)$$

where q_t (mmol g^{-1}) is the amount of CO_2 adsorbed per mass of sorbent at the time t, and k_f (min^{-1}) is the rate constant of first-order sorption. Once integrated with the boundary conditions t =0, q_t =0 and t = ∞, $q_t = q_e$ it gives:

$$q_t = q_e\left[1 - exp\left(-k_f t\right)\right] \quad (7)$$

This model can properly describe a reversible type of adsorbate/adsorbent interactions, as the case of CO_2 adsorption on physical adsorbents like activated carbons and zeolites [58].

The pseudo-second order kinetic model was firstly proposed by Blanchard et al. [59] and it assumes that the adsorption rate is proportional to the square of the number of available adsorption sites on the adsorbent surface. Its mathematical expression in the differential form is [59]:

$$\frac{dq_t}{dt} = k_s(q_e - q_t)^2 \quad (8)$$

where k_s (g $mmol^{-1}$ min^{-1}) is the second order rate constant. Integrating and applying boundary conditions t =0, qt = 0, and t = ∞, $q_t = q_e$, Eq. (8) becomes:

$$q_t = \frac{{q_e}^2 k_s t}{1 + q_e k_s t} \quad (9)$$

This model assumes that, besides weak physical interactions, adsorption is also associated to chemical adsorbate/adsorbent interactions, thus being generally most suited to describe chemisorption [59].

The fitting quality of the kinetic models to the experimental data has been then assessed by evaluating the coefficient of regression, R^2, and the he hybrid fractional error function (HYBRID) as in Eq (4).

Once computed the kinetic constant, the activation energy (E_a), defined as the minimum energy that must be overcome by the adsorbate molecules [64], has been calculated through the Arrhenius equation [31].

5. Results and discussion

5.1 Materials characterization

The XRD patterns of the samples are shown in Figure 2. The samples are characterized by a rather high level of cristallinity, with characteristic reflection peaks of chabazite located at 2θ=20.45, 22.86, 24.61, 30.40, and 30.73 [65], typically abundant in natural zeolites, together with other impurities (feldspar, quartz, calcite, etc.) [66]. From the comparison of the XRD patterns (Figure 2a and b) it can be inferred that the phase composition does not vary remarkably when the sample was conditioned at 250 °C, thus meaning that the material is quite stable in the low and medium temperature range.

Detailed information regarding the morphology, chemical composition and pore distribution of the tuff can be found elsewhere [26], also including SEM and N_2 adsorption characterization. Briefly, the material is characterized by micronic cubic shaped structures, typical of the zeolites, as well as glassy regions, and it is basically microporous (7 Å < d < 20 Å) with a unimodal pore size distribution, as typically reported for zeolites.

5.2 Breakthrough curves

Figures 3a and b report the breakthrough curves obtained at 25°C for all the adopted CO_2 inlet concentrations, and with an inlet CO_2 concentration of 10% vol. for all the adopted adsorption temperatures, respectively. The adsorption results in terms of adsorption isotherms and adsorption parameters are shown in Figure 4 and Table 2. It can be inferred that temperature and pressure have different effects on the CO_2 adsorption process depending on whether the process is observed from the thermodynamic or the kinetic point of view.

The CO_2 adsorption capacity q_e, i.e. the amount of CO_2 adsorbed once the thermodynamic equilibrium is reached, is enhanced as P_{CO2} is increased, which is in accordance with the fact that P_{CO2} is the adsorption driving force from the thermodynamic point of view. On the contrary, q_e decreases as the temperature is increased (i.e. the adsorption isotherms become less and less favorable), which is in agreement with the adsorption exothermicity. Indeed, when the temperature is increased more energy is conveyed to the CO_2 molecules in the gaseous phase, which means in turns that CO_2 diffusion takes place faster. On the other hand, however, the more excited CO_2 molecules are less prone to be trapped on the sorbent surface. As a matter of fact, at higher temperatures, the adsorbed CO_2 can more easily move back to the gaseous phase since they have enough energy to escape from the attraction forces exerted by the adsorbent surface and the CO_2 molecules already in the gaseous phase tend to stay there [40].

Looking at the process from the kinetic point of view, both temperature and P_{CO2} positively affect the CO_2 adsorption rate (the process becomes faster, i.e. the time needed to achieve the equilibrium becomes smaller), as clearly confirmed by the decrease of $\Delta\tau$ and the increase of ψ as either temperature or P_{CO2} pressure is increased. This is also clearly shown by the breakthrough curves becoming steeper and steeper as either temperature or P_{CO2} increased (Figure 3). As regards the adsorption temperature, this can be ascribed to the fact that faster mass-transfer phenomena take place at higher temperature due to the molecule mobility being enhanced [67]. Likewise, when P_{CO2} is increased, the adsorption becomes faster, which is basically ascribable to the enhancement of the mass transfer rate as a result of the higher adsorption driving force [67]. As a matter of fact, lower CO_2 partial pressures result in slower breakthrough curves due to the CO_2 concentration front taking more time to reach the outlet of the bed [5,32,56]. Also this result is in agreement with several works available in the literature on CO_2 adsorption on physical sorbents [5,32,56].

On the contrary, t_b is negatively affected by both temperature and P_{CO2}, as it decreases as either of them is increased. As regards the effect of temperature, this is due to the fact that when temperature

is increased, the adsorption capacity is reduced and the adsorption rate is increased, which both lead to a faster saturation of the bed. A more complex discussion must be devoted to the effect of P_{CO2}, which is the result of the combination of two opposed phenomena. On the one hand, as discussed above, from a thermodynamic point of view, the increased P_{CO2} results in an enhanced adsorption uptake of the sorbent; as a consequence, t_b is also increased. On the other hand, higher values of P_{CO2} lead to a faster adsorption process, which in turns results in a faster saturation of the sorbent and, consequently, in a decrease of t_b. Therefore all these things considered, the latter aspect prevails on the first.

5.3 Adsorption thermodynamics

5.3.1 Adsorption isotherms

The fitting of the experimental data by Langmuir and Freundlich models are reported in Figures 4a and b, respectively. The marker points represent the experimental data while the solid lines represent the results of isotherm models. Table 3 reports the values of the model parameters, R^2 and HYBRID.

Figure 4 clearly shows that both the models used in this work fitted the experimental results quite well, in line with the results obtained by other Authors with physical sorbents [37–45]. This was also confirmed by the fact that R^2 is always larger than 0.99 and HYBRID is always lower than 0.5%. As a matter of fact, it is quite common that both Langmuir and Freundlich isotherms are able to fairly fit the same set of CO_2 adsorption data at certain CO_2 partial pressure ranges, at least from a macroscopic point of view [68–70]. In particular, this is true especially when P_{CO2} is small (i.e. < 0.1atm, as typical of post- combustion capture applications) and q_e is also small enough to have linear shape of adsorption isotherm. As a confirmation, it clearly appears from Figure 4a that the Langmuir fitting is less accurate at lower temperatures, i.e. when q_e is larger and the adsorption isotherms moves away from the linearity (i.e. Freundlich is by far the best model to describe CO_2

adsorption on the natural tuff at lower temperatures). This can be ascribed to the fact that when a larger amount of CO_2 is adsorbed, it is most likely that multiple layers of CO_2 molecules are adsorbed on the sorbent surface; as a consequence, Freundlich model is able to give a better fitting [48].

As regards the effect of temperature, Table 3 clearly shows that, when temperature is increased, the predicted values of maximum amount of CO_2 adsorbed (q_L) and adsorption isotherm constants (K_L and K_F,) decreased. This is in line with the exothermicity of the CO_2 adsorption phenomenon on the tuff, i.e. it is thermodynamically favored at low temperatures (this is also confirmed by an increase of temperature, about 4-5 °C, registered during the adsorption tests). Indeed, when the temperature is reduced, more CO_2 molecules are adsorbed on the tuff surface; as a consequence, the competition among CO_2 molecules for the limited number of still available adsorption sites is stronger (also resulting from the stronger repulsion forces among the molecules themselves), thus leading to a general decrease of adsorption intensity [40].

Also regarding the results obtained from the Freundlich model $n > 1$ at all the investigated temperatures, which is an indication of a high level of heterogeneity of the system as long as of good adsorption intensity [48,71,72]. Also, the dependence of n on the adsorption temperature is a further confirmation of the fact that CO_2 adsorption on the tuff is favored at low temperatures, in accordance with its exothermic in nature.

As regards the Langmuir model, Figure 5 shows the calculated values of the separation factor, R_L, for different temperatures as a function of P_{CO2}. R_L is always < 1, which confirms that CO_2 uptake is favorable using the natural tuff sorbent. Besides, the decrease of R_L with increasing values of P_{CO2} shows that adsorption is less reversible at higher P_{CO2}. From a practical point of view, the CO_2 uptake at low temperatures and P_{CO2} up to 0.10 atm, i.e. reasonable conditions for post-combustion capture, would have R_L not lower than 0.75.

Figure 6 shows the CH_4 adsorption isotherm obtained at 25 °C; the CO_2 adsorption isotherm has also been reported for comparison. In line with data reported in literature for zeolites [34], CO_2 is adsorbed in a much larger amount than CH_4., approaching a maximum selectivity factor of 8.7 at P_i=0.01 atm that slightly decreases down to 7.7 at Pi=0.20 atm (see inset in Fig. 6). The selectivity factor results quite good, only lower to that of purposely synthetized sorbents, e.g. 13X zeolite, geopolymers, amine compounds [17]. This results can be explained considering that the tested tuff has been found to be characterized by a rather high level of cristallinity, with characteristic reflection peaks of chabazite. Chabazite (structural formula $(Ca_2,Na_4,K_4)[(AlO_2)_4(SiO_2)_8]$ $13H_2O$) has a three-dimensional framework delimited by eight-membered rings that create pore openings of 0.38 nm, i.e. very close to the kinetic dimension of CH_4 (0.38 nm) [73–76]. Then, considering that the kinetic dimension of CO_2 (0.33 nm) is remarkably smaller than CH_4, chabazite and chabazite-like zeolites (and also other 8 rings zeolites) can be used as selective adsorbents for CO_2 from natural gas. As a matter of fact, they can allow for a kinetically enhanced CO_2-over-CH_4 selectivity [73–76]. This finding also confirms the results reported for another natural tuff by Paolini et al. [29], reinforcing the idea to use the natural tuff as potential sorbent to be easily applied in landfill gas purification, CO_2 removal from natural gas and biogas upgrading.

5.3.2 Evaluation of thermodynamic properties

Figure 7 reports van't Hoff plot for the natural tuff in the temperature range of 25 - 150 °C. The values of ΔH^0, ΔS^0 and ΔG^0, calculated from the slope ($\Delta H^0/R$) and intercept ($\Delta S^0/R$) of the plot and from Eq. (8) are listed in Table 4.

ΔG^0 is always negative, thus indicating that the CO_2 adsorption process on the tuff occurs favorably and spontaneously at all the adopted adsorption temperatures. Besides that, the van't Hoff plot exhibits an increasing trend; i.e. when temperature is increased, the magnitude of ΔG^0 is decreased (ΔG^0 becomes less negative), which is a confirmation of the adsorption feasibility decreasing at higher temperatures. This result can be ascribed to the fact that, at higher

temperatures, the physical bonds between CO_2 molecules and adsorbent become weaker and the reverse of adsorption (i.e. desorption) is favored; namely there is a shift of the equilibrium in the opposite direction, i.e. from adsorption to desorption [64].

Besides that, lower temperatures favored also a better interaction of CO_2 with the tuff particles due to the lower kinetic energy of CO_2 molecules, thus favoring the multilayer adsorption of CO_2 molecules [77,78]. This is also in line with the above reported adsorption isotherms.

The value obtained for ΔH^0 is about -17 kJ mol^{-1}. First of all, its negative sign further confirms the exothermicity of the adsorption process, i.e. energy in form of heat is generated into its surroundings during the adsorptive process since new physical/chemical bonds are formed. Besides that, its magnitude gives also further insight into the adsorption mechanism. In particular, ΔH^0 values are lower than 20 kJ mol^{-1}, thus confirming that CO_2 adsorption on the tuff is physical in nature [50].

Finally, ΔS^0 is also negative, meaning that the disorder and randomness of the system decrease during the adsorption process. This can be ascribed to the fact that, when adsorbed on the tuff surface, the CO_2 molecules lose the freedom of movement they have in the gaseous phase; in other words, CO_2 molecules pass from a random state (gas) to an ordered state (on the tuff surface) [40].

Figure 8 shows the adsorption isosteres of the yellow tuff, i.e. plots of $\ln(P_{CO2})$ as a function of reciprocal absolute temperature at constant loading, 0.05-1 mmol g^{-1}, in the investigated temperature range 25 -150 °C. Then, applying the Clausius–Clapeyron equation, Q_{st} was evaluated from the slopes (Q_{st}/R) of the above-mentioned isosteres. All the isosteres exhibit negative slopes, which is consistent with the CO_2 adsorption being exothermic.

Then, the magnitude and change of Q_{st} during CO_2 adsorption (i.e. with the surface loading increasing) can provide information on the molecular-scale interactions between the CO_2 molecules and the adsorbent and also on the energetic heterogeneity of the solid surface [46]. The obtained values of Q_{st} were plotted as a function of the equilibrium surface loading in Figure 9. First of all,

the yellow tuff exhibits values of Q_{st} ranging between 15 and 45 kJ mol^{-1} that are typical of a purely physical interaction (< 80 kJ mol^{-1}) [40].

Then, it is clear that Q_{st}, i.e. the slope of the adsorption isosteres, decreases with increasing CO_2 surface loading, which means that the tuff is characterized by a high level of heterogeneity and that there is a variation in adsorbate-adsorbent and adsorbate-adsorbate interactions [79]. In general, Q_{st} is associated with the interaction between CO_2 molecules and the adsorbent surface through different kinds of adsorptive molecular forces, such as Van der Waals forces, hydrophobicity, ligand exchange and chemical bond [80]. At the initial stages of adsorption, large numbers of free adsorption sites are available on the tuff surface. As a consequence, the CO_2 molecules may easily come into direct contact with adsorbent surface, more intense forces being present between CO_2 molecules and the adsorbent; as a consequence, the activation energy is low and the heat of adsorption is high. As the adsorption process goes further, i.e. the surface coverage is increased, less and less adsorption sites are still available and, as a consequence, the adsorption of further CO_2 molecules becomes more and more difficult. Besides that, with the surface coverage increasing, also adsorbate–adsorbate interactions start to occur. Therefore, it is most likely that some kind of lateral interactions in the adsorbed layers take place in the form of attractive/repulsive London dispersion intermolecular forces between adsorbed CO_2 [79,81,82]. As a result, as the adsorption process proceeds, the activation energy is increased and the heat of adsorption is decreased [83,84].

5.4 Adsorption kinetics

Figure 10a reports the CO_2 transient adsorption uptakes on the tuff at different adsorption temperatures (at 10%vol. of CO_2 inlet concentration), as evaluated from the experimental breakthrough curves. The same curves have been also plotted as fractional uptake (q_t/q_e) (Figure 10b) in order to better highlight the effect of the temperature.

The analysis of Figure 10 clearly shows that adsorption kinetics and thermodynamics are differently affected by the temperature. Indeed, when temperature is increased, the CO_2 adsorption

becomes faster due to enhanced kinetics and, on the contrary, the amount of CO_2 adsorbed at equilibrium is decreased due to thermodynamics limitation. In other words, the equilibrium CO_2 adsorption capacity decreases with the temperature increasing (i.e. the asymptotic values reached by the CO_2 uptake curves in Figure 10a has a decreasing trend as temperatures increased), which is in line with the exothermicity of the adsorption. On the contrary, higher temperatures positively affect adsorption kinetics (i.e. the time needed to achieve the equilibrium becomes smaller), as it is clearly shown by the curves becoming steeper (Figure 10b) with increasing temperatures, in accordance with the fastened mass-transfer and diffusion phenomena at higher values of adsorption temperatures.

Then, the pseudo-first order and pseudo-second order models have been used to fit the experimental data. Figure 11 reports the comparison between the experimental and theoretical curves, the points representing the experimental values whereas the dashed lines the amounts predicted by the kinetic models. Table 5 reports the values of the kinetic constants with the relative correlation coefficients and errors.

Figure 11 clearly shows that for each investigated temperature, the pseudo-first order kinetic model fits the experimental data better than the pseudo-second order kinetic model does (this shows larger deviations from the experimental data). More specifically, the pseudo-second order model tends to underestimate the CO_2 uptake in the first few minutes ($t < 5$ min); in contrast, this is remarkably overestimated in the last stage of the adsorption process, namely as the equilibrium is approaching. As a consequence, the pseudo-second order model significantly overestimates the equilibrium CO_2 uptake (q_e) (Table 5). In contrast to this, the pseudo-first kinetic model is capable of adequately fitting the experimental points during the entire time evolution of the adsorption. This better quality is clearly confirmed by the data reported in Table 5, in terms of higher values of R^2 and lower values of HYB (%).

These results can be ascribed to the fact that that the pseudo-first order can fairly describe adsorption processes characterized by reversible adsorbate/adsorbent surface interactions, i.e. purely physical adsorption. On the contrary, the second-order kinetic model can better describe chemisorption processes, i.e. it is a better choice when it is necessary to account for the occurrence of chemical bonding between the adsorbate and the adsorbent surface. Therefore, these results are in line with those obtained from the thermodynamic study, showing that the CO_2 adsorption on the tuff is purely physisorption. This is also in accordance with several works available in literature, reporting that the pseudo-first order kinetic model is more suitable for adsorption on physical sorbents at post-combustion operating conditions, i.e. at low CO_2 partial pressure [55].

It can also be also observed that, whatever the kinetic model, the kinetic constant (k_f and k_s) increase with increasing temperatures, which is in line with high temperatures favoring the adsorption process (Table 5).

Considering the suitability of the pseudo-first order kinetic model, the corresponding kinetic coefficients at various temperatures have been used to evaluate the activation energy and pre-exponential factor of an Arrhenius type equation by a linear regression on its linearized form [31]. Figure 12 shows the plots of the linearized Arrhenius equation. $E_a > 0$, meaning that when the temperature is increased, the reaction rate is increased. More specifically, the value obtained (14.4 kJ/mol) is in line with data available in other works focused on zeolites [85]. This quite small value confirms again the physical adsorption with the relatively weak attraction forces.

6. Assessment of the process performance

The results obtained with the yellow tuff trigger some speculations about possible application in a real process for CO_2 capture in a post-combustion scheme.

First of all the purity of the separated carbon dioxide is dictated by the ratio between the useful volume V_{CO_2} for selective CO_2 adsorption and "dead volume" V_d, where the original gas mixture may remain entrapped. Apart from intrinsic dead volumes in the plant setup (e.g. valves, tubing,

manifolds), the inter-particle voids and, in some extent, the particle macro-porosity represent major source of "dead volume". For a bed of granular sorbent, the volume of the separated CO_2 is given by:

$$V_{CO_2} = q_e \frac{R\,T}{P} V_r \rho_e (1-\varepsilon) \quad (9)$$

Where, V_r, ρ_e and ε are the vessel volume, the envelope or particle density and the bed voidage, respectively. Assuming only the contribution of the inter-particle voids, the dead volume in the adsorption equipment is $V_d = \varepsilon V_r$. Thus, the volumetric concentration C_{CO2} of the separated CO_2 can be calculated from the species conservation equation:

$$C_{CO_2} = \frac{V_d C^0_{CO2} + 100\, V_{CO_2}}{V_d + V_{CO_2}} \quad (10)$$

where, $C^0_{CO_2}$ is the inlet CO_2 concentration. The following expression, giving the theoretical purity of the separated carbon dioxide, can be obtained by substitution:

$$\frac{C_{CO_2}}{100} = \frac{\varepsilon C^0_{CO_2}/100 + q_e \frac{R\,T}{P} \rho_e (1-\varepsilon)}{\varepsilon + q_e \frac{R\,T}{P} \rho_e (1-\varepsilon)} \quad (11)$$

The purity increases at lower voidage, higher inlet concentration, and lower temperature because of the non-linear dependence of q_e on T.

For the case of the yellow tuff, assuming the values of the properties reported in Table 1 and 2 at atmospheric pressure, the purity turns out to be equal to 0.975 and 0.966, at temperature of 25 and 70 °C, respectively. It is worth noting that in a CCS process the minimum purity should be 0.96, in consideration of the constrain for gas delivery and in presence of non-condensable gases in the separated stream [86]. Thus, the studied sorbent complies with the criterion of the CO_2 purity for CCS.

As second speculation, the energy required for the sorbent regeneration was taken into account. To this aim both temperature swing (TS) and/or vacuum swing (VS) procedures have been considered. In the case of TS, the enthalpy penalty H_t, per unit mass of separated carbon dioxide,

was computed (Eq. 12) as the heat required for heating the sorbent up to the regeneration temperature T_r plus the latent heat of the adsorbed CO_2, λ being the molar enthalpy of adsorption:

$$H_t = \frac{C(T_r - T)}{0.044\, q_e} + 0.044\, \lambda \quad (12)$$

In the case of VS, two different penalties are present, the first being again H_t (Eq. 12), the second being the work W_e for evacuating the sorbent from CO_2. In particular, W_e has been calculated assuming the conservative case of isentropic compression from the absolute vacuum level P_v to atmospheric pressure according to:

$$W_e = \frac{R}{\gamma - 1} \frac{(T - T_{ad})}{0.044} \quad (13)$$

where, T_{ad} and γ are the adiabatic temperature and isentropic expansion factor for poly-atomic gas, respectively. In turn, T_{ad} is computed as:

$$T_{ad} = T \left(\frac{1}{P_v}\right)^{\gamma - 1} \quad (14)$$

For a case study of 1 MW_t power plant fired with coal, the sorbent rate was evaluated on the basis of the emitted CO_2 in the flue gas and that captured in the regenerated sorbent, also taking into account the partial utilization of this latter. Eq.15 expresses the virtual mass flow rate of the sorbent $\dot{m}_s$ that linearly depends on the carbon content in the fuel (X_C), and the inverse of sorbent capacity q_e and utilization ψ, 28 MJ kg^{-1} and 0.012 kg mol^{-1} being the coal heating value and the carbon atomic weight, respectively:

$$\dot{m}_s = \frac{1}{28} X_C \frac{1}{0.012\, \psi\, q_e} \quad (15)$$

It is worth noting that in real cases the sorbent is kept in static conditions. Thus it only virtually circulates between CO_2 capture and regeneration reactors; indeed these steps are accomplished by alternatively switching the gaseous streams in coupled vessels.

The results of calculations are reported in Table 6, assuming a concentration of CO_2 in flue gas equal to 15 % vol that is typical of a coal fueled power plant.

Four different cases are reported in the table at different adsorption temperature (cols. 1-3), and for a sorbent with double capacity with respect to yellow tuff (col. 4). Three regeneration strategies are compared: a) temperature swing, b) vacuum swing and c) temperature and vacuum swing in cascade.

It appears that in case of TS (a) the sorbent rate is the lowest, thanks to the higher regeneration temperature (105 °C) that better evacuates the sorbent. In contrast, the energy penalty H_t is very high and obviously W_e is null. For the vacuum swing method (b) the enthalpy penalty H_t is only the latent heat for CO_2 desorption, whilst negative work W_e is required because of the gas compression from 0.05 to 1.00 atm. The sorbent rates are higher than in case (a). The case (c) is a cascade of TS at 70 °C followed by VS from 0.10 to 1.00 atm. In this case, the work request is lower than for (b), being the CO_2 evacuated under less severe condition. The shaded cells denote a good compromise between temperature and pressure swing for CO_2 capture with yellow tuff.

When the adsorption capacity of the sorbent is increased (cols. 1 vs. 4), obviously the comparison turns out favorable for the more performing sorbent, whose rate largely decreased. However, in the case of VS only (b) the same enthalpy penalty and work are foreseen (i.e. H_t=0.041 MJ/kg, W_e=-0.288 MJ/kg), since these depend on the captured carbon dioxide only. Altogether, a sorbent with limited CO_2 capture capacity would be more conveniently employed in VS or combined TS and VS modes, in order to minimize the whole energy penalties.

7. Conclusions

In this work CO_2 adsorption on a natural tuff has been studied focusing on the thermodynamics and kinetics of the process. Dynamic breakthrough experiments have been performed in a lab-scale fixed bed reactor.

As regards thermodynamics, it is oppositely affected by temperature and pressure. Indeed, when CO_2 partial pressure is increased, the equilibrium CO_2 adsorption uptake increases, whereas it decreases when temperature is increased. The equilibrium experimental data have been fitted by

Langmuir and Freundlich models. The Freundlich model provides the better results in terms of fitting quality, which suggests that CO_2 adsorption on the tuff is multilayer and happens with a heterogeneous surface binding (the adsorption energy exhibits by a non-uniform distribution). Then, the study of the thermodynamic parameters has shown that CO_2 adsorption on the tuff is spontaneous, exothermic and physical in nature. As the surface loading increase the isosteric heat of adsorption decreases, which is a further confirmation of the fact that the tuff has an energetically heterogeneous surface and that some kind of lateral interactions take place among the CO_2 molecules adsorbed on the tuff surface.

Then, the pseudo-first and pseudo-second kinetic model have been adopted to fit the experimental data. The pseudo-first order kinetic model is the best one, being able to provide a better quality of the fitting all the investigated adsorption temperatures. The values of activation energy, evaluated from the obtained kinetic coefficients, further confirmed that the CO_2 adsorption process is physical in nature.

The yellow tuff is also characterized by quite good CO_2/CH_4 equilibrium selectivity, thus being potentially applied also in landfill gas purification, CO_2 removal from natural gas and biogas upgrading, where larger concentration of carbon dioxide occurs.

In the framework of a possible application in a real process for post-combustion CO_2 capture, it can be speculated that the natural tuff, i.e. a sorbent with limited CO_2 capture capacity with respect to other more performing materials, could be more conveniently employed in vacuum swing or mixed mode, thus minimizing the energy penalty of the process.

Acknowledgement

Mr. A. Piancastelli is gratefully acknowledged for MIP and XRD analyses on tuff samples.

References

[1] P. Ammendola, R. Chirone, G. Ruoppolo, G. Russo, Production of hydrogen from thermo-catalytic decomposition of methane in a fluidized bed reactor, Chem. Eng. J. 154 (2009) 287–294. doi:10.1016/j.cej.2009.03.048.

[2] D.Y.C. Leung, G. Caramanna, M.M. Maroto-Valer, An overview of current status of carbon dioxide capture and storage technologies, Renew. Sustain. Energy Rev. 39 (2014) 426–443. doi:10.1016/j.rser.2014.07.093.

[3] A. Samanta, A. Zhao, G.K.H. Shimizu, P. Sarkar, R. Gupta, Post-Combustion CO2 Capture Using Solid Sorbents: A Review, Ind. Eng. Chem. Res. 51 (2012) 1438–1463. doi:10.1021/ie200686q.

[4] M. Karl, R.F. Wright, T.F. Berglen, B. Denby, Worst case scenario study to assess the environmental impact of amine emissions from a CO2 capture plant, Int. J. Greenh. Gas Control. 5 (2011) 439–447. doi:10.1016/j.ijggc.2010.11.001.

[5] M.G. Plaza, S. García, F. Rubiera, J.J. Pis, C. Pevida, Post-combustion CO2 capture with a commercial activated carbon: Comparison of different regeneration strategies, Chem. Eng. J. 163 (2010) 41–47. doi:10.1016/j.cej.2010.07.030.

[6] M. Alfe, P. Ammendola, V. Gargiulo, F. Raganati, R. Chirone, Magnetite loaded carbon fine particles as low-cost CO2 adsorbent in a sound assisted fluidized bed, Proc. Combust. Inst. 35 (2015) 2801–2809. doi:10.1016/j.proci.2014.06.037.

[7] P. Ammendola, F. Raganati, R. Chirone, Effect of operating conditions on the CO2 recovery from a fine activated carbon by means of TSA in a fluidized bed assisted by acoustic fields, Fuel Process. Technol. 134 (2015) 494–501. doi:10.1016/j.fuproc.2015.03.010.

[8] F. Raganati, P. Ammendola, R. Chirone, On improving the CO2 recovery efficiency of a conventional TSA process in a sound assisted fluidized bed by separating heating and purging, Sep. Purif. Technol. 167 (2016) 24–31. doi:10.1016/j.seppur.2016.05.001.

[9] F. Raganati, P. Ammendola, R. Chirone, Effect of acoustic field on CO2 desorption in a fluidized bed of fine activated carbon, Particuology. 23 (2015) 8–15. doi:10.1016/j.partic.2015.02.001.

[10] F. Raganati, P. Ammendola, R. Chirone, Role of Acoustic Fields in Promoting the Gas-Solid Contact in a Fluidized Bed of Fine Particles, KONA Powder Part. J. 32 (2015) 23–40. doi:10.14356/kona.2015006.

[11] V. Gargiulo, M. Alfè, P. Ammendola, F. Raganati, R. Chirone, CO2 sorption on surface-modified carbonaceous support: Probing the influence of the carbon black microporosity and surface polarity, Appl. Surf. Sci. 360 (2016) 329–337. doi:10.1016/j.apsusc.2015.11.026.

[12] M. Hemmat, A. Rahbar-Kelishami, M.H. Vakili, Preparation of carbon molecular sieves and its impregnation with Co and Ni for CO2/N2 separation, Int. J. Environ. Sci. Technol. 15 (2018) 2213–2228. doi:10.1007/s13762-017-1526-5.

[13] F. Raganati, P. Ammendola, R. Chirone, CO2 capture performances of fine solid sorbents in a sound-assisted fluidized bed, Powder Technol. 268 (2014) 347–356. doi:10.1016/j.powtec.2014.08.062.

[14] R. Girimonte, B. Formisani, F. Testa, Adsorption of CO2 on a confined fluidized bed of pelletized 13X zeolite, Powder Technol. 311 (2017) 9–17. doi:10.1016/j.powtec.2017.01.033.

[15] S.C. Lee, Y.M. Kwon, C.Y. Ryu, H.J. Chae, D. Ragupathy, S.Y. Jung, J.B. Lee, C.K. Ryu,

J.C. Kim, Development of new alumina-modified sorbents for CO2 sorption and regeneration at temperatures below 200°C, Fuel. (2010) 2–7. doi:10.1016/j.fuel.2010.11.006.

[16] K.B. Lee, M.G. Beaver, H.S. Caram, S. Sircar, Reversible Chemisorbents for Carbon Dioxide and Their Potential Applications, Ind. Eng. Chem. Res. 47 (2008) 8048–8062. doi:10.1021/ie800795y.

[17] M. Minelli, E. Papa, V. Medri, F. Miccio, P. Benito, F. Doghieri, E. Landi, Characterization of novel geopolymer – Zeolite composites as solid adsorbents for CO2 capture, Chem. Eng. J. 341 (2018) 505–515. doi:10.1016/j.cej.2018.02.050.

[18] M. Minelli, V. Medri, E. Papa, F. Miccio, E. Landi, F. Doghieri, Geopolymers as solid adsorbent for CO2 capture, Chem. Eng. Sci. 148 (2016) 267–274. doi:10.1016/j.ces.2016.04.013.

[19] M.G. Plaza, C. Pevida, J.J. Pis, F. Rubiera, Evaluation of the cyclic capacity of low-cost carbon adsorbents for post-combustion CO2 capture, Energy Procedia. 4 (2011) 1228–1234. doi:10.1016/j.egypro.2011.01.178.

[20] M. Sevilla, J.B. Parra, A.B. Fuertes, Assessment of the role of micropore size and N-doping in CO2 capture by porous carbons., ACS Appl. Mater. Interfaces. 5 (2013) 6360–8. doi:10.1021/am401423b.

[21] F. Raganati, V. Gargiulo, P. Ammendola, M. Alfe, R. Chirone, CO2 capture performance of HKUST-1 in a sound assisted fluidized bed, Chem. Eng. J. 239 (2014) 75–86. doi:10.1016/j.cej.2013.11.005.

[22] V. Gargiulo, M. Alfè, F. Raganati, L. Lisi, R. Chirone, P. Ammendola, BTC-based metal-organic frameworks: Correlation between relevant structural features and CO2 adsorption performances, Fuel. 222 (2018) 319–326. doi:10.1016/j.fuel.2018.02.093.

[23] R. V. Siriwardane, M.-S. Shen, E.P. Fisher, J.A. Poston, Adsorption of CO2 on Molecular Sieves and Activated Carbon, Energy & Fuels. 15 (2001) 279–284. doi:10.1021/ef000241s.

[24] N. Gargiulo, K. Shibata, A. Peluso, P. Aprea, T. Valente, G. Pezzotti, T. Shiono, D. Caputo, Reinventing rice husk ash: derived NaX zeolite as a high-performing CO2 adsorbent, Int. J. Environ. Sci. Technol. 15 (2018) 1543–1550. doi:10.1007/s13762-017-1534-5.

[25] M. Ackley, R. Rege, H. Saxena, Application of natural zeolites in the purification and separation of gases, Microporous Mesoporous Mater. 61 (2003) 25–42. doi:10.1016/S1387-1811(03)00353-6.

[26] P. Ammendola, F. Raganati, R. Chirone, F. Miccio, Preliminary Assessment of Tuff as CO2 Sorbent, Energy Procedia. 114 (2017) 46–52. doi:10.1016/j.egypro.2017.03.1145.

[27] P. Misaelides, Application of natural zeolites in environmental remediation: A short review, Microporous Mesoporous Mater. 144 (2011) 15–18. doi:10.1016/j.micromeso.2011.03.024.

[28] C. Colella, Applications of Natural Zeolites, in: Handb. Porous Solids, Wiley-VCH Verlag GmbH, Weinheim, Germany, 2008: pp. 1156–1189. doi:10.1002/9783527618286.ch18i.

[29] V. Paolini, F. Petracchini, E. Guerriero, A. Bencini, S. Drigo, Biogas cleaning and upgrading with natural zeolites from tuffs, Environ. Technol. 37 (2016) 1418–1427.

doi:10.1080/09593330.2015.1118557.

[30] A. Alonso-Vicario, J.R. Ochoa-Gómez, S. Gil-Río, O. Gómez-Jiménez-Aberasturi, C.A. Ramírez-López, J. Torrecilla-Soria, A. Domínguez, Purification and upgrading of biogas by pressure swing adsorption on synthetic and natural zeolites, Microporous Mesoporous Mater. 134 (2010) 100–107. doi:10.1016/j.micromeso.2010.05.014.

[31] P. Ammendola, F. Raganati, R. Chirone, CO2 adsorption on a fine activated carbon in a sound assisted fluidized bed: Thermodynamics and kinetics, Chem. Eng. J. 322 (2017) 302–313. doi:10.1016/j.cej.2017.04.037.

[32] F. Raganati, M. Alfe, V. Gargiulo, R. Chirone, P. Ammendola, Isotherms and thermodynamics of CO2 adsorption on a novel carbon-magnetite composite sorbent, Chem. Eng. Res. Des. 134 (2018) 540–552. doi:10.1016/j.cherd.2018.04.037.

[33] D. Geldart, Gas fluidization technology, Wiley & Son, Chichester; New York, 1986.

[34] N.K. Jensen, T.E. Rufford, G. Watson, D.K. Zhang, K.I. Chan, E.F. May, Screening Zeolites for Gas Separation Applications Involving Methane, Nitrogen, and Carbon Dioxide, J. Chem. Eng. Data. 57 (2012) 106–113. doi:10.1021/je200817w.

[35] M.V. Gil, N. Álvarez-Gutiérrez, M. Martínez, F. Rubiera, C. Pevida, A. Morán, Carbon adsorbents for CO2 capture from bio-hydrogen and biogas streams: Breakthrough adsorption study, Chem. Eng. J. 269 (2015) 148–158. doi:10.1016/j.cej.2015.01.100.

[36] F. Raganati, M. Alfe, V. Gargiulo, R. Chirone, P. Ammendola, Kinetic study and breakthrough analysis of the hybrid physical/chemical CO2 adsorption/desorption behavior of a magnetite-based sorbent, Chem. Eng. J. 372 (2019) 526–535. doi:10.1016/j.cej.2019.04.165.

[37] B. Guo, L. Chang, K. Xie, Adsorption of Carbon Dioxide on Activated Carbon, J. Nat. Gas Chem. 15 (2006) 223–229. doi:10.1016/S1003-9953(06)60030-3.

[38] B. Selen, A.˘ Glayan, A.E. Aksoylu, CO2 adsorption behavior and kinetics on chemically modified activated carbons, Turk J Chem. 40 (2016) 576–587. doi:10.3906/kim-1507-95.

[39] J. Sreńscek-Nazzal, U. Narkiewicz, A.W. Morawski, R. Wróbel, A. Gęsikiewicz-Puchalska, B. Michalkiewicz, Modification of Commercial Activated Carbons for CO 2 Adsorption, Acta Phys. Pol. A. 129 (2016) 394–401. doi:10.12693/APhysPolA.129.394.

[40] X. Zhou, H. Yi, X. Tang, H. Deng, H. Liu, Thermodynamics for the adsorption of SO2, NO and CO2 from flue gas on activated carbon fiber, Chem. Eng. J. 200–202 (2012) 399–404. doi:10.1016/j.cej.2012.06.013.

[41] A. Golchoobi, H. Pahlavanzadeh, Molecular simulation, experiments and modelling of single adsorption capacity of 4A molecular sieve for CO 2 –CH 4 separation, Sep. Sci. Technol. 51 (2016) 2318–2325. doi:10.1080/01496395.2016.1206571.

[42] J.-S. Lee, J.-H. Kim, J.-T. Kim, J.-K. Suh, J.-M. Lee, C.-H. Lee, Adsorption Equilibria of CO 2 on Zeolite 13X and Zeolite X/Activated Carbon Composite, J. Chem. Eng. Data. 47 (2002) 1237–1242. doi:10.1021/je020050e.

[43] X. Xu, X. Zhao, L. Sun, X. Liu, Adsorption separation of carbon dioxide, methane, and

nitrogen on Hβ and Na-exchanged β-zeolite, J. Nat. Gas Chem. 17 (2008) 391–396. doi:10.1016/S1003-9953(09)60015-3.

[44] M.A. Hernandez, A. Pestryakov, R. Portillo, M.A. Salgado, F. Rojas, E. Rubio, S. Ruiz, V. Petranovskii, CO2 Sequestration by Natural Zeolite for Greenhouse Effect Control, Procedia Chem. 15 (2015) 33–41. doi:10.1016/j.proche.2015.10.006.

[45] L. Hauchhum, P. Mahanta, Carbon dioxide adsorption on zeolites and activated carbon by pressure swing adsorption in a fixed bed, Int. J. Energy Environ. Eng. 5 (2014) 349–356. doi:10.1007/s40095-014-0131-3.

[46] M. Saleh Shafeeyan, W. Mohd Ashri Wan Daud, A. Shamiri, N. Aghamohammadi, Adsorption equilibrium of carbon dioxide on ammonia-modified activated carbon, Chem. Eng. Res. Des. 104 (2015) 42–52. doi:10.1016/j.cherd.2015.07.018.

[47] I. Langmuir, The constitution and fundamental properties of solids and liquids. Part I. Solids, J. Am. Chem. Soc. 38 (1916) 2221–2295. doi:10.1021/ja02268a002.

[48] M.F. Freundlich, Over the adsorption in solution, J. Phys. Chem. 57 (1906) 355–471.

[49] D. Tiwari, C. Goel, H. Bhunia, P.K. Bajpai, Dynamic CO2 capture by carbon adsorbents: Kinetics, isotherm and thermodynamic studies, Sep. Purif. Technol. 181 (2017) 107–122. doi:10.1016/j.seppur.2017.03.014.

[50] A.A. Adelodun, J.C. Ngila, D.-G. Kim, Y.-M. Jo, Isotherm, Thermodynamic and Kinetic Studies of Selective CO2 Adsorption on Chemically Modified Carbon Surfaces, Aerosol Air Qual. Res. 16 (2016) 3312–3329. doi:10.4209/aaqr.2016.01.0014.

[51] D. Iruretagoyena Ferrer, Supported Layered Double Hydroxides as CO2 Adsorbents for Sorption-enhanced H2 Production, Springer International Publishing, Cham, 2016. doi:10.1007/978-3-319-41276-4.

[52] J. a. Mason, K. Sumida, Z.R. Herm, R. Krishna, J.R. Long, Evaluating metal–organic frameworks for post-combustion carbon dioxide capture via temperature swing adsorption, Energy Environ. Sci. 4 (2011) 3030–3040. doi:10.1039/c1ee01720a.

[53] S.-C. Hsu, C. Lu, F. Su, W. Zeng, W. Chen, Thermodynamics and regeneration studies of CO2 adsorption on multiwalled carbon nanotubes, Chem. Eng. Sci. 65 (2010) 1354–1361. doi:10.1016/j.ces.2009.10.005.

[54] S. Loganathan, M. Tikmani, S. Edubilli, A. Mishra, A.K. Ghoshal, CO2 adsorption kinetics on mesoporous silica under wide range of pressure and temperature, Chem. Eng. J. 256 (2014) 1–8. doi:10.1016/j.cej.2014.06.091.

[55] R. Serna-Guerrero, A. Sayari, Modeling adsorption of CO2 on amine-functionalized mesoporous silica. 2: Kinetics and breakthrough curves, Chem. Eng. J. 161 (2010) 182–190. doi:10.1016/j.cej.2010.04.042.

[56] N. Álvarez-Gutiérrez, M.V. Gil, F. Rubiera, C. Pevida, Kinetics of CO2 adsorption on cherry stone-based carbons in CO2/CH4 separations, Chem. Eng. J. 307 (2017) 249–257. doi:10.1016/j.cej.2016.08.077.

[57] C. Goel, H. Kaur, H. Bhunia, P.K. Bajpai, Carbon dioxide adsorption on nitrogen enriched

carbon adsorbents: Experimental, kinetics, isothermal and thermodynamic studies, J. CO2 Util. 16 (2016) 50–63. doi:10.1016/j.jcou.2016.06.002.

[58] S.Y. Lagergren, Zur Theorie der sogenannten Adsorption gelöster Stoffe, K. Sven. Vetenskapsakad. Handl. 24 (1898) 1–39.

[59] G. Blanchard, M. Maunaye, G. Martin, Removal of heavy metals from waters by means of natural zeolites, Water Res. 18 (1984) 1501–1507. doi:10.1016/0043-1354(84)90124-6.

[60] Y.S. Ho, G. McKay, Kinetic model for lead(II) sorption on to peat, Adsorpt. Sci. Technol. (1998). doi:10.1177/026361749801600401.

[61] Y.S. Ho, G. McKay, A Comparison of Chemisorption Kinetic Models Applied to Pollutant Removal on Various Sorbents, Process Saf. Environ. Prot. 76 (1998) 332–340. doi:10.1205/095758298529696.

[62] M.A. Hubbe, S. Azizian, S. Douven, Implications of Apparent Pseudo-Second-Order Adsorption Kinetics onto Cellulosic Materials: A Review, BioResource. 14 (2019) 7582–7626.

[63] G. Song, X. Zhu, R. Chen, Q. Liao, Y.-D. Ding, L. Chen, An investigation of CO2 adsorption kinetics on porous magnesium oxide, Chem. Eng. J. 283 (2016) 175–183. doi:10.1016/j.cej.2015.07.055.

[64] H.N. Tran, S.-J. You, H.-P. Chao, Thermodynamic parameters of cadmium adsorption onto orange peel calculated from various methods: A comparison study, J. Environ. Chem. Eng. 4 (2016) 2671–2682. doi:10.1016/j.jece.2016.05.009.

[65] M.M.J. Treacy, J.B. Higgins, Collection of Simulated XRD Powder Patterns for Zeolites, Elsevier, 2001.

[66] R. Leyva-Ramos, J.E. Monsivais-Rocha, A. Aragon-Piña, M.S. Berber-Mendoza, R.M. Guerrero-Coronado, P. Alonso-Davila, J. Mendoza-Barron, Removal of ammonium from aqueous solution by ion exchange on natural and modified chabazite, J. Environ. Manage. 91 (2010) 2662–2668. doi:10.1016/j.jenvman.2010.07.035.

[67] D.M. Ruthven, Principles of adsorption and adsorption processes, John Wiley & Sons, 1984.

[68] E.R. Monazam, L.J. Shadle, D.C. Miller, H.W. Pennline, D.J. Fauth, J.S. Hoffman, M.L. Gray, Equilibrium and kinetics analysis of carbon dioxide capture using immobilized amine on a mesoporous silica, AIChE J. 59 (2013) 923–935. doi:10.1002/aic.13870.

[69] J. Sreńscek-Nazzal, U. Narkiewicz, A.W. Morawski, R.J. Wróbel, B. Michalkiewicz, Comparison of Optimized Isotherm Models and Error Functions for Carbon Dioxide Adsorption on Activated Carbon, J. Chem. Eng. Data. 60 (2015) 3148–3158. doi:10.1021/acs.jced.5b00294.

[70] H. Yi, H. Deng, X. Tang, Q. Yu, X. Zhou, H. Liu, Adsorption equilibrium and kinetics for SO2, NO, CO2 on zeolites FAU and LTA, J. Hazard. Mater. 203–204 (2012) 111–117. doi:10.1016/j.jhazmat.2011.11.091.

[71] R. Sips, On the Structure of a Catalyst Surface, J. Chem. Phys. 16 (1948) 490–495. doi:10.1063/1.1746922.

[72] J. Toth, State Equations of the Solid-Gas Interface Layers, Acta Chim. Acad. Sci. Hungaricae. 69 (1971) 311–328.

[73] J. Shang, G. Li, R. Singh, Q. Gu, K.M. Nairn, T.J. Bastow, N. Medhekar, C.M. Doherty, A.J. Hill, J.Z. Liu, P.A. Webley, Discriminative Separation of Gases by a "Molecular Trapdoor" Mechanism in Chabazite Zeolites, J. Am. Chem. Soc. 134 (2012) 29. doi:10.1021/ja309274y.

[74] T. De Baerdemaeker, D. De Vos, Trapdoors in zeolites, Nat. Chem. 5 (2013) 89–90. doi:10.1038/nchem.1560.

[75] G.C. Watson, N.K. Jensen, T.E. Rufford, K.I. Chan, E.F. May, Volumetric Adsorption Measurements of N 2 , CO 2 , CH 4 , and a CO 2 + CH 4 Mixture on a Natural Chabazite from (5 to 3000) kPa, J. Chem. Eng. Data. 57 (2012) 93–101. doi:10.1021/je200812y.

[76] Z. Bacsik, O. Cheung, P. Vasiliev, N. Hedin, Selective separation of CO2 and CH4 for biogas upgrading on zeolite NaKA and SAPO-56, Appl. Energy. 162 (2016) 613–621. doi:10.1016/j.apenergy.2015.10.109.

[77] A.K. Mishra, S. Ramaprabhu, Magnetite decorated graphite nanoplatelets as cost effective CO2 adsorbent, J. Mater. Chem. 21 (2011) 7467. doi:10.1039/c1jm10996k.

[78] A.K. Mishra, S. Ramaprabhu, Nano magnetite decorated multiwalled carbon nanotubes: a robust nanomaterial for enhanced carbon dioxide adsorption, Energy Environ. Sci. 4 (2011) 889–895. doi:10.1039/C0EE00076K.

[79] V.K. Singh, E. Anil Kumar, Measurement and analysis of adsorption isotherms of CO2 on activated carbon, Appl. Therm. Eng. 97 (2016) 77–86. doi:10.1016/j.applthermaleng.2015.10.052.

[80] A. Heydari-Gorji, A. Sayari, CO2 capture on polyethylenimine-impregnated hydrophobic mesoporous silica: Experimental and kinetic modeling, Chem. Eng. J. 173 (2011) 72–79. doi:10.1016/j.cej.2011.07.038.

[81] Y. Belmabkhout, A. Sayari, Effect of pore expansion and amine functionalization of mesoporous silica on CO2 adsorption over a wide range of conditions, Adsorption. 15 (2009) 318–328. doi:10.1007/s10450-009-9185-6.

[82] A. Koide, T. Kihara, Intermolecular forces for D2, N2, O2, F2 and CO2, Chem. Phys. (1974). doi:10.1016/0301-0104(74)80004-2.

[83] S. Himeno, T. Tomita, K. Suzuki, S. Yoshida, Characterization and selectivity for methane and carbon dioxide adsorption on the all-silica DD3R zeolite, Microporous Mesoporous Mater. 98 (2007) 62–69. doi:10.1016/j.micromeso.2006.05.018.

[84] P. Ning, F. Li, H. Yi, X. Tang, J. Peng, Y. Li, D. He, H. Deng, Adsorption equilibrium of methane and carbon dioxide on microwave-activated carbon, Sep. Purif. Technol. 98 (2012) 321–326. doi:10.1016/j.seppur.2012.07.001.

[85] V.K. Singh, E.A. Kumar, Comparative Studies on CO2 Adsorption Kinetics by Solid Adsorbents, Energy Procedia. 90 (2016) 316–325. doi:10.1016/j.egypro.2016.11.199.

[86] E. de Visser, C. Hendriks, M. Barrio, M.J. Mølnvik, G. de Koeijer, S. Liljemark, Y. Le Gallo, Dynamis CO2 quality recommendations, Int. J. Greenh. Gas Control. 2 (2008) 478–

484. doi:10.1016/j.ijggc.2008.04.006.

Figure captions

Figure 1. Experimental apparatus: 1) N_2 cylinder; 2) CO_2 cylinder; 3) N_2 mass flow controller; 4) CO_2 mas flow controller; 5) multichannel control instrument; 6) 6 mm ID fixed bed reactor; 7) thermocouple; 8) temperature controller; 9) heating jacket; 10) CO_2 analyzer; 11) stack.

Figure 2. XRD patterns of the yellow tuff after drying at 100 °C (a) and after treatment at 250 °C (b).

Figure 3. Breakthrough curves for CO_2 adsorption on the natural tuff: a) at a fixed adsorption temperature of 25°C and varying the inlet CO_2 concentration; b) at a fixed inlet CO_2 concentration of 10%vol. and varying the adsorption temperature.

Figure 4. Adsorption isotherms of CO_2 on the natural tuff at different adsorption temperatures fitted by: a) Langmuir model; b) Freundlich model.

Figure 5. Separation factor as function of CO_2 partial pressure.

Figure 6. Adsorption isotherms of CH_4 and CO_2 on the natural tuff obtained at 25 °C. P_i = partial pressure of CH_4 and CO_2 in the CH_4/N_2 and CO_2/N_2 mixtures, respectively.

Figure 7. Van't Hoff plot.

Figure 8. Adsorption isosteres of CO_2 on the natural tuff. Adsorption temperature range: 25 - 150 °C; CO_2 loading: 0.05 - 1.00 mmol g^{-1}.

Figure 9. Variation of the isosteric heat of adsorption with the CO_2 loading.

Figure 10. a) CO_2 transient adsorption uptakes; b) CO_2 fractional adsorption uptakes.

Figure 11. Experimental (dotted line) CO_2 uptake on the natural tuff and corresponding fit to the pseudo-first (solid line) and pseudo-second (dashed line) order kinetic models at different adsorption temperatures.

Figure 12. Arrhenius plot: logarithm of the kinetic constant versus inverse of absolute temperature.

Table captions

Table 1. Physical properties of the natural tuff.

Table 2. Results of CO_2 adsorption tests on the natural tuff.

Table 3. Langmuir and Freundlich adsorption equation parameters and fitting comparison.

Table 4. Thermodynamic properties for CO_2 adsorption on the natural tuff.

Table 5. Values of the pseudo-first order and pseudo-second kinetic model parameters and fitting comparison.

Table 6. Sorbent rate and energy penalties for CO_2 capture.

Figure(s)

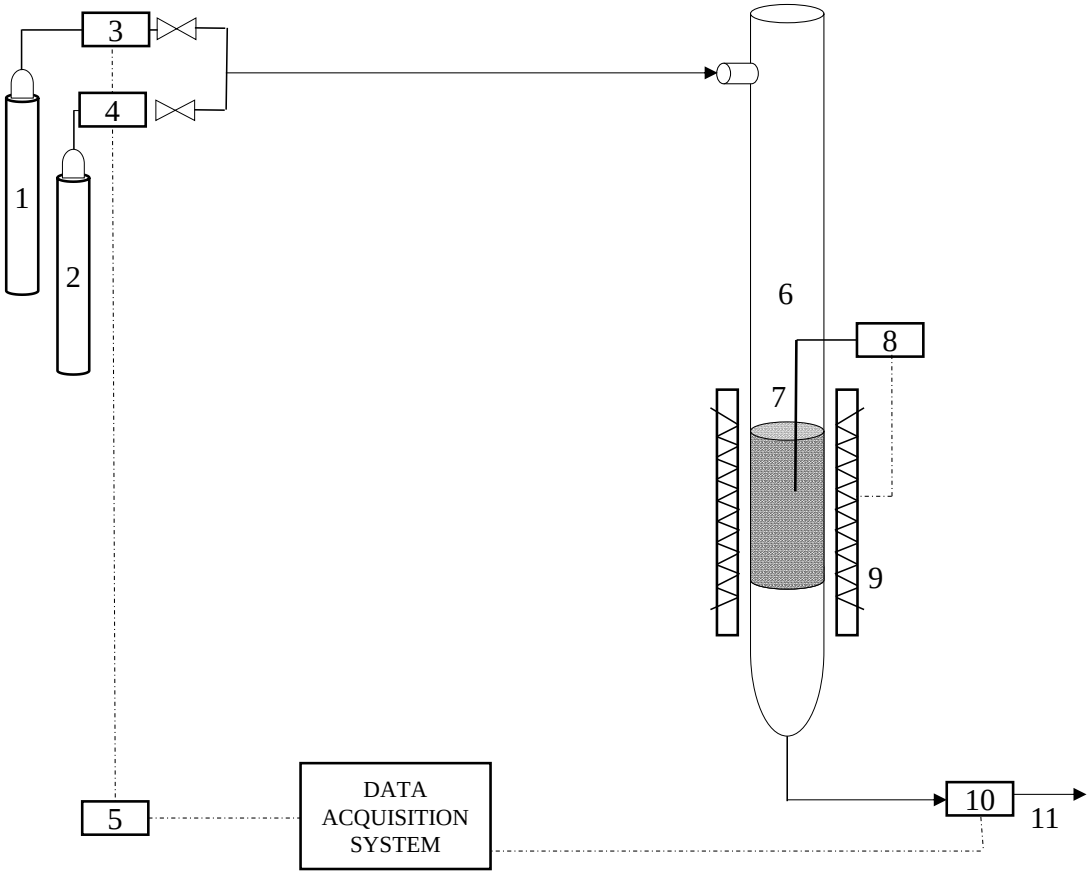

Fig. 1. Experimental apparatus: 1) N_2 cylinder; 2) CO_2 cylinder; 3) N_2 mass flow controller; 4) CO_2 mas flow controller; 5) multichannel control instrument; 6) 6 mm ID fixed bed reactor; 7) thermocouple; 8) temperature controller; 9) heating jacket; 10) CO_2 analyzer; 11) stack.

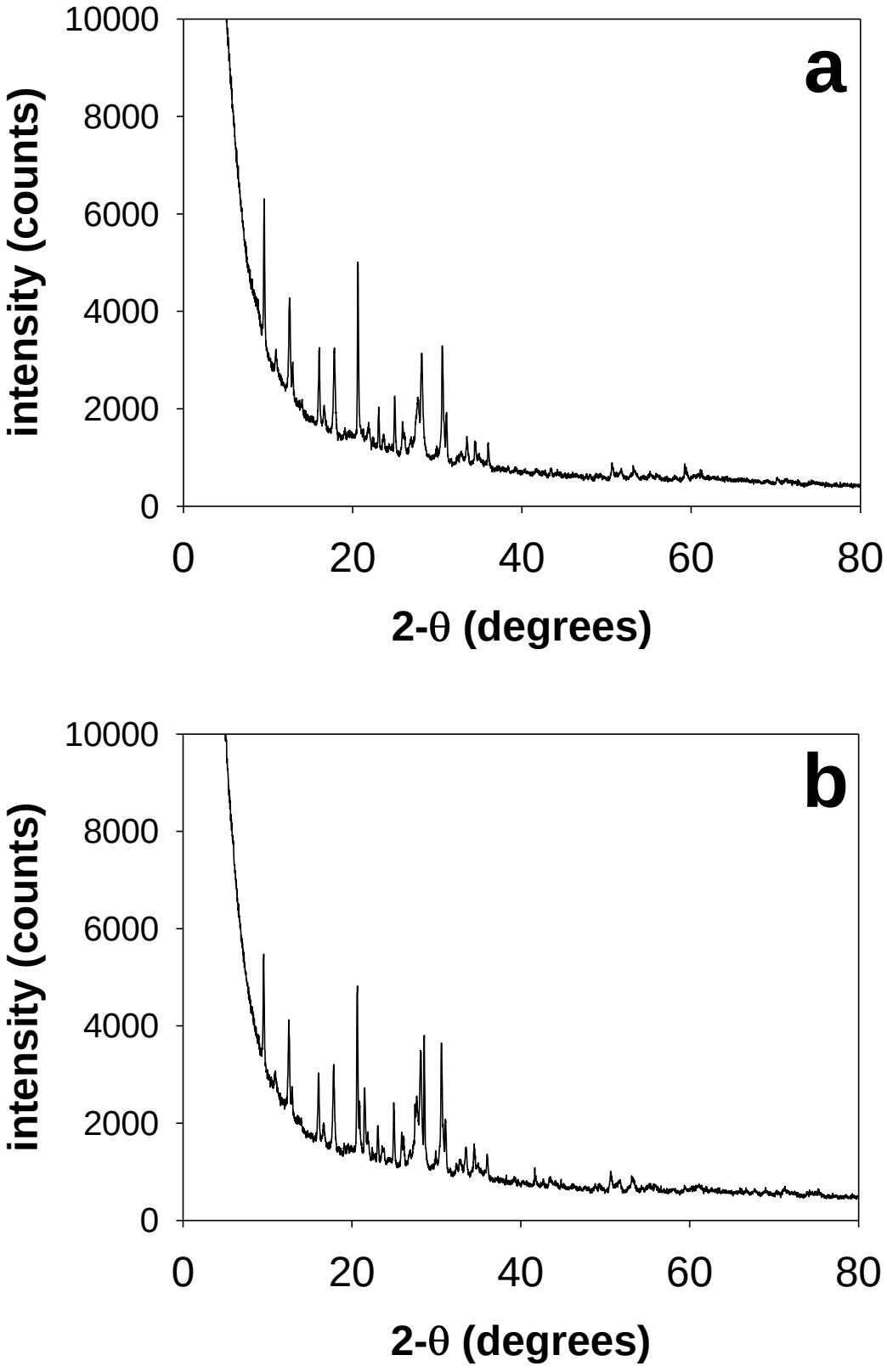

Fig. 2. XRD patterns of the yellow tuff after drying at 100 °C (a) and after treatment at 250 °C (b).

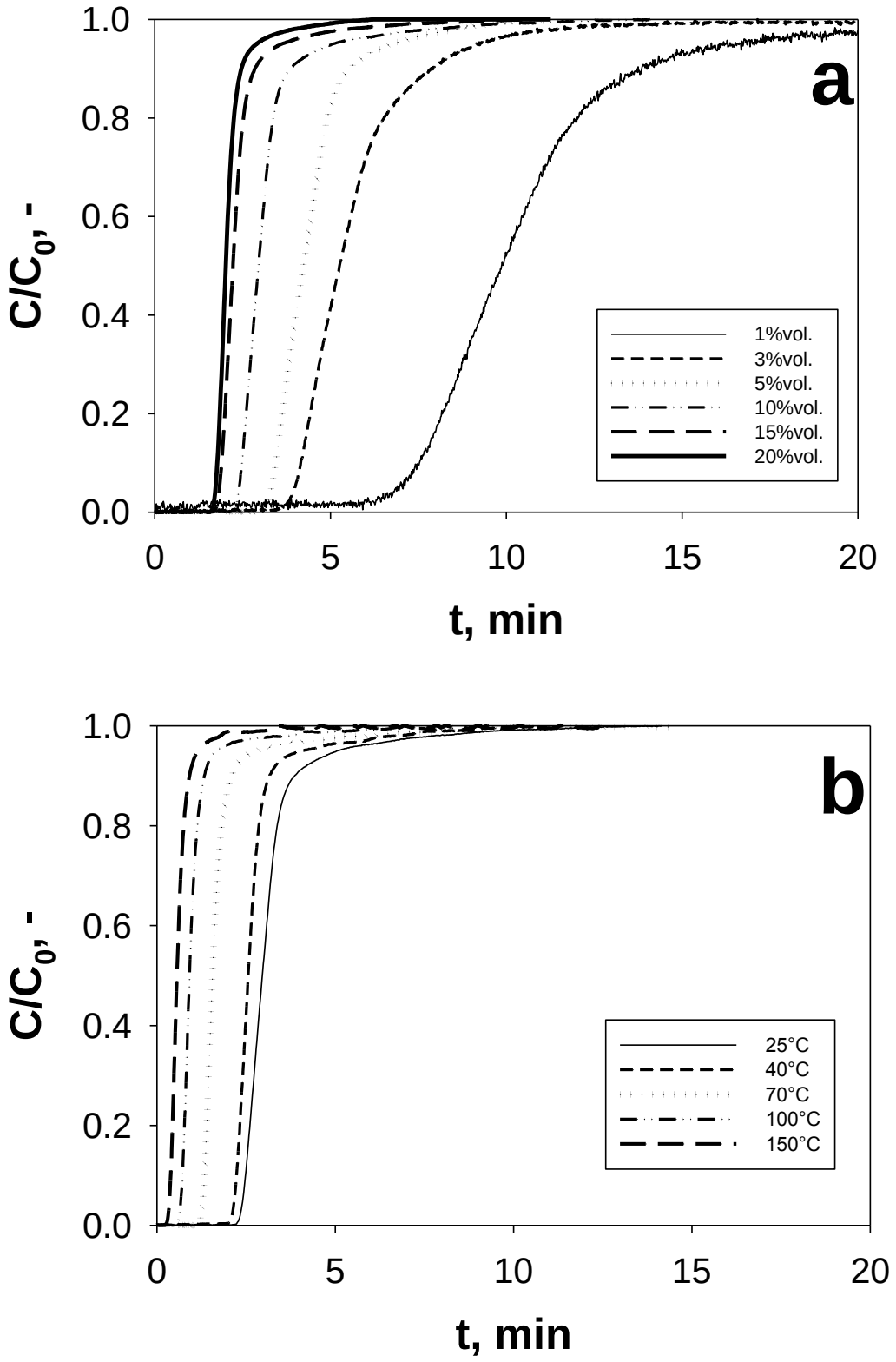

Fig. 3. Breakthrough curves for CO_2 adsorption on the natural tuff: a) at a fixed adsorption temperature of 25°C and varying the inlet CO_2 concentration; b) at a fixed inlet CO_2 concentration of 10%vol. and varying the adsorption temperature.

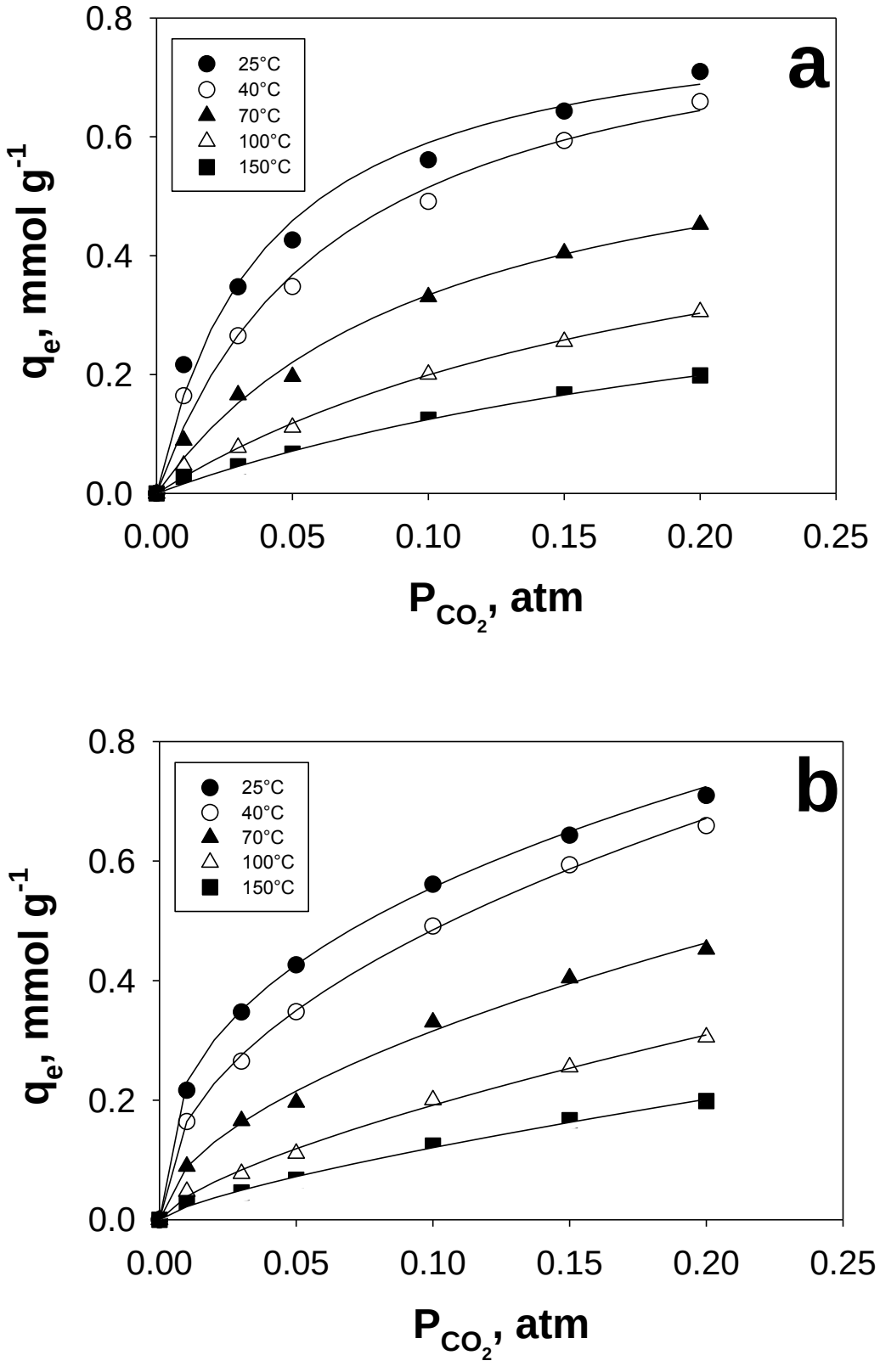

Fig. 4. Adsorption isotherms of CO_2 on the natural tuff at different adsorption temperatures fitted by: a) Langmuir model; b) Freundlich model.

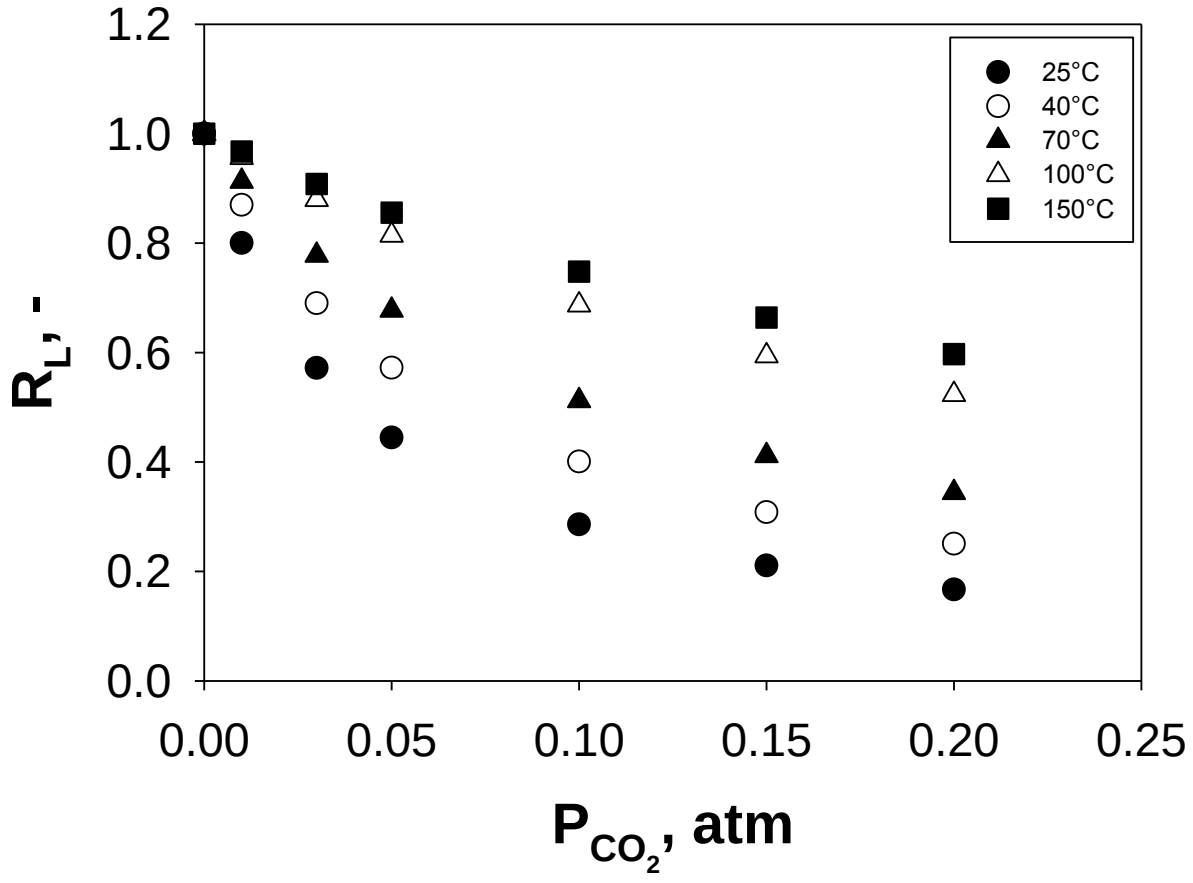

Fig. 5. Separation factor as function of CO_2 partial pressure.

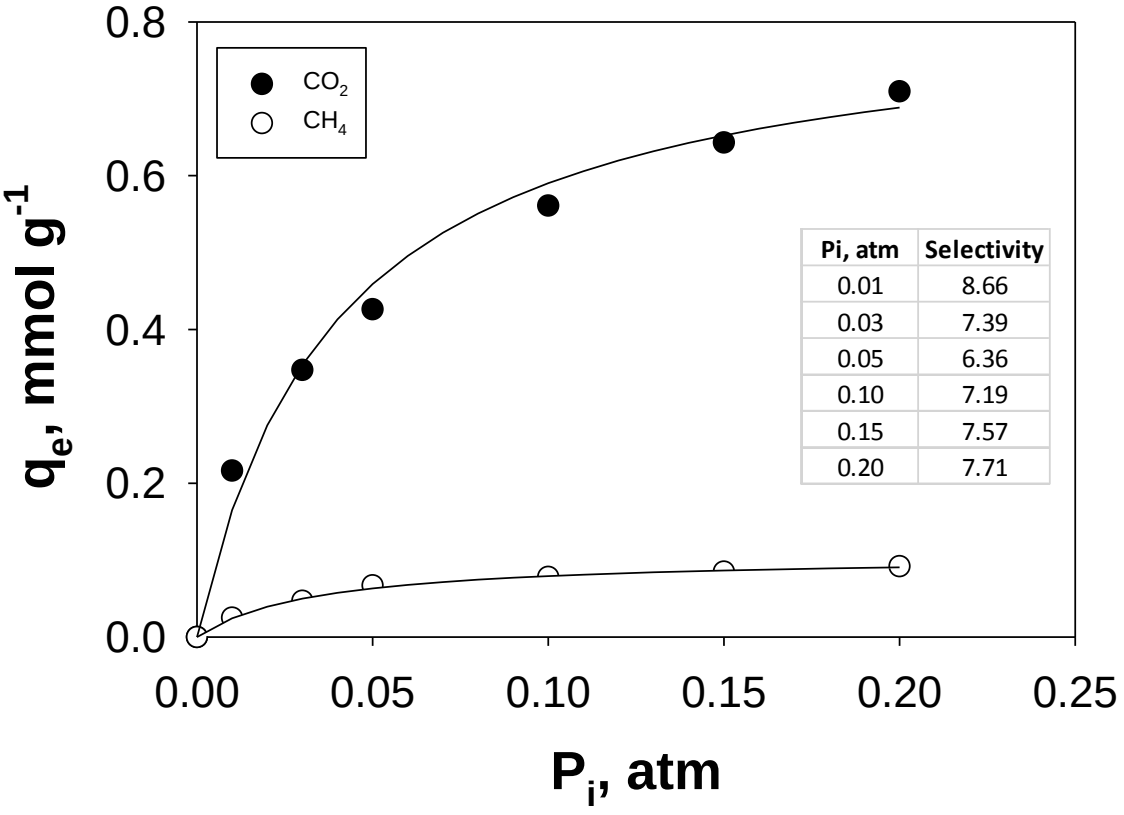

Figure 6. Adsorption isotherms of CH_4 and CO_2 on the natural tuff obtained at 25 °C. P_i = partial pressure of CH_4 and CO_2 in the CH_4/N_2 and CO_2/N_2 mixtures, respectively.

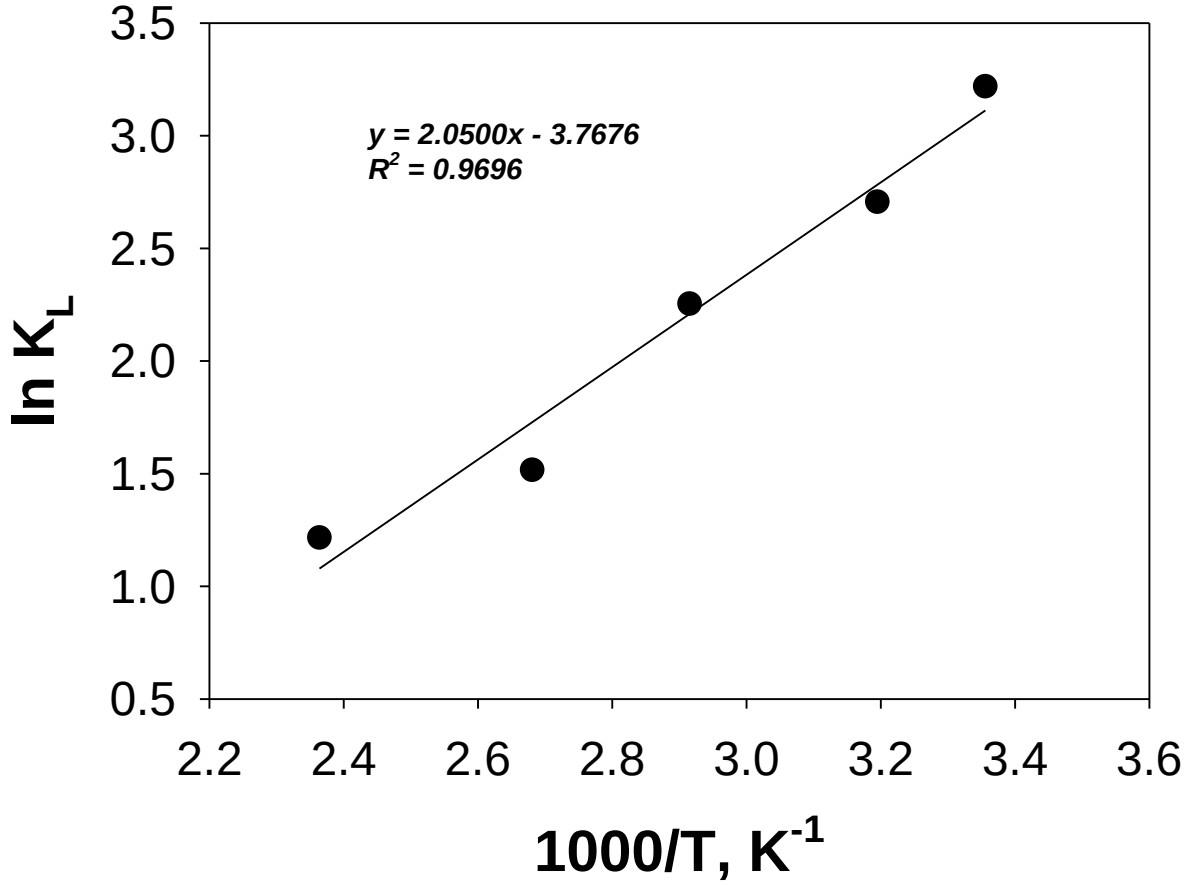

Fig. 7. Van't Hoff plot.

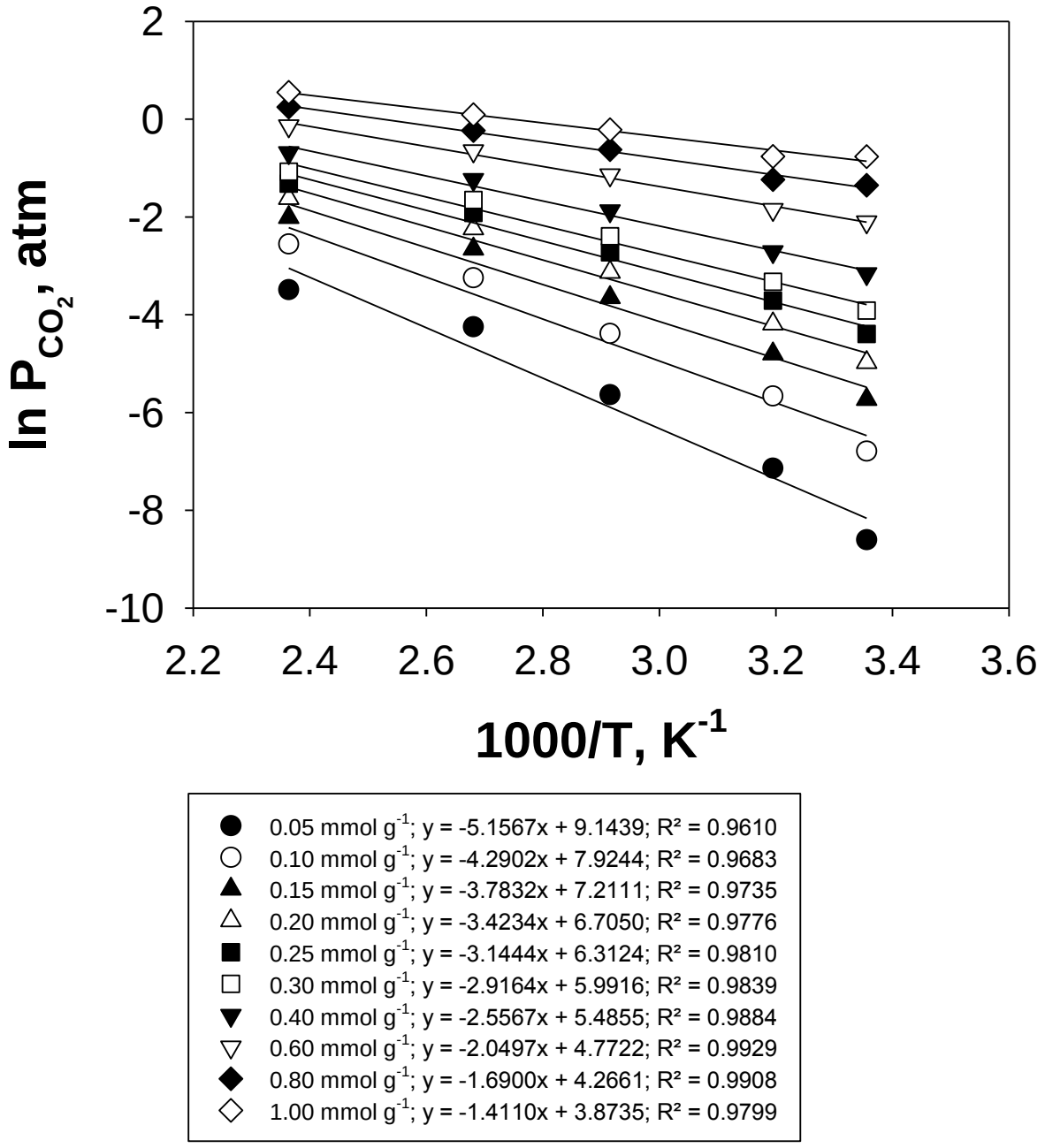

Fig. 8. Adsorption isosteres of CO_2 on the natural tuff. Adsorption temperature range: 25 - 150 °C; CO_2 loading: 0.05 - 1.00 mmol g^{-1}.

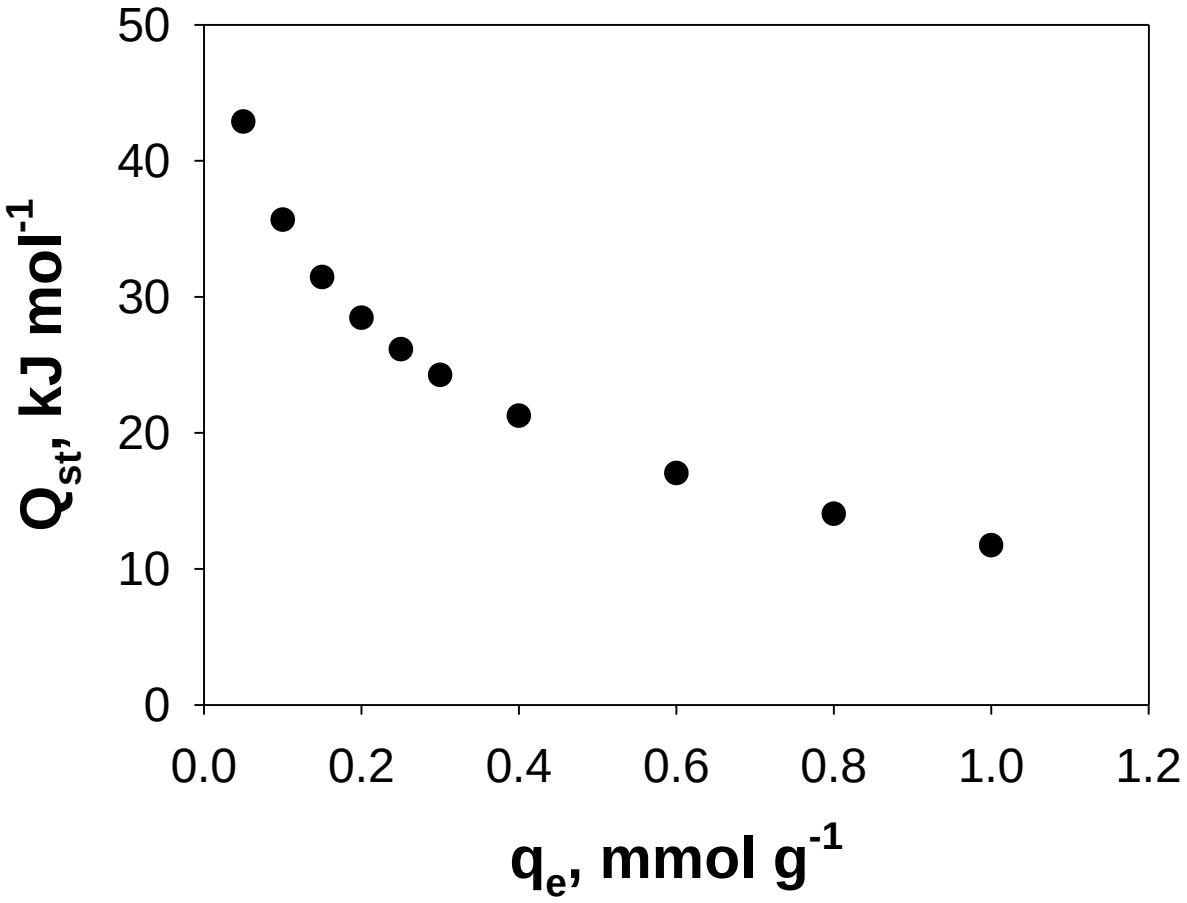

Fig. 9. Variation of the isosteric heat of adsorption with the CO_2 loading.

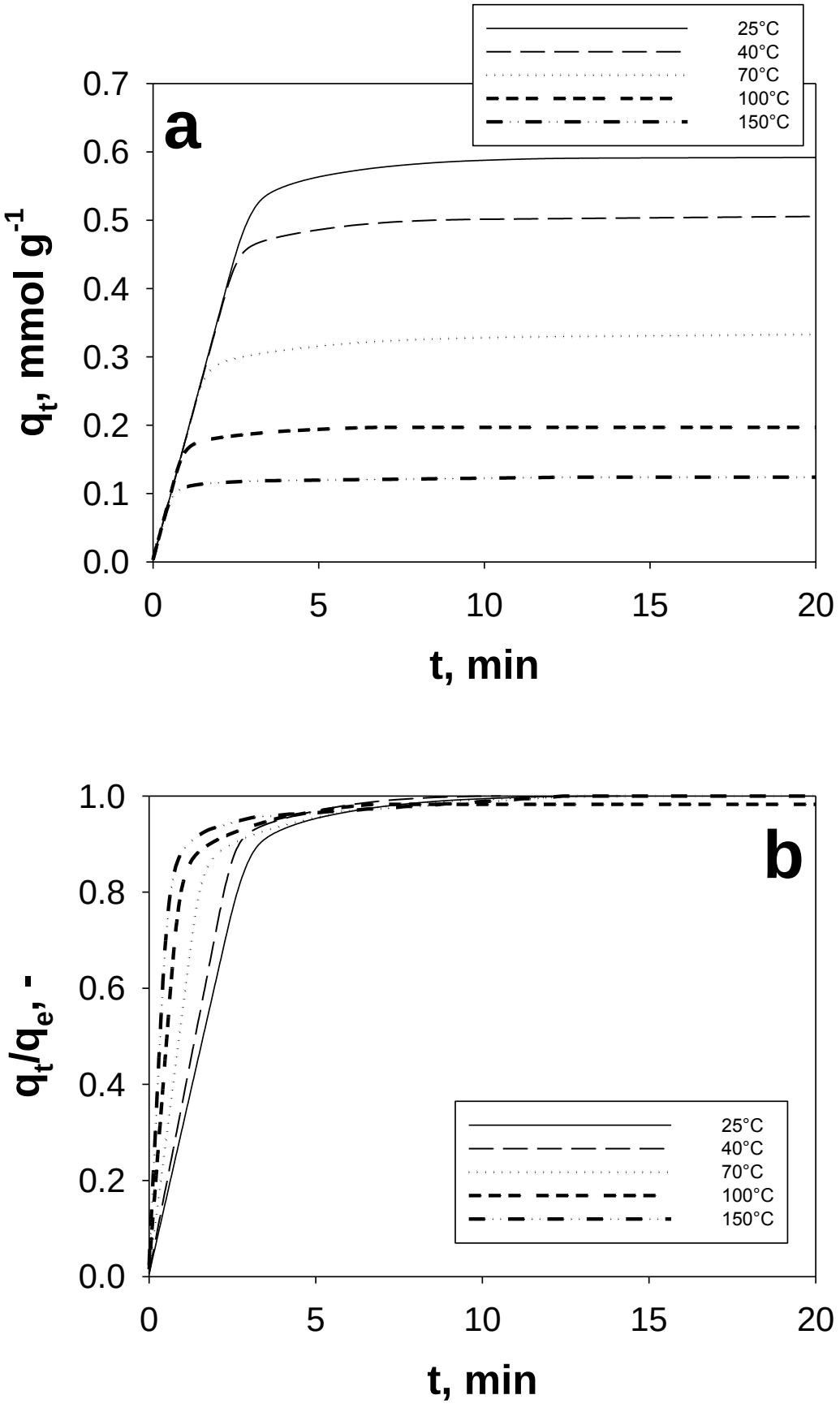

Fig. 10. a) CO_2 transient adsorption uptakes; b) CO_2 fractional adsorption uptakes.

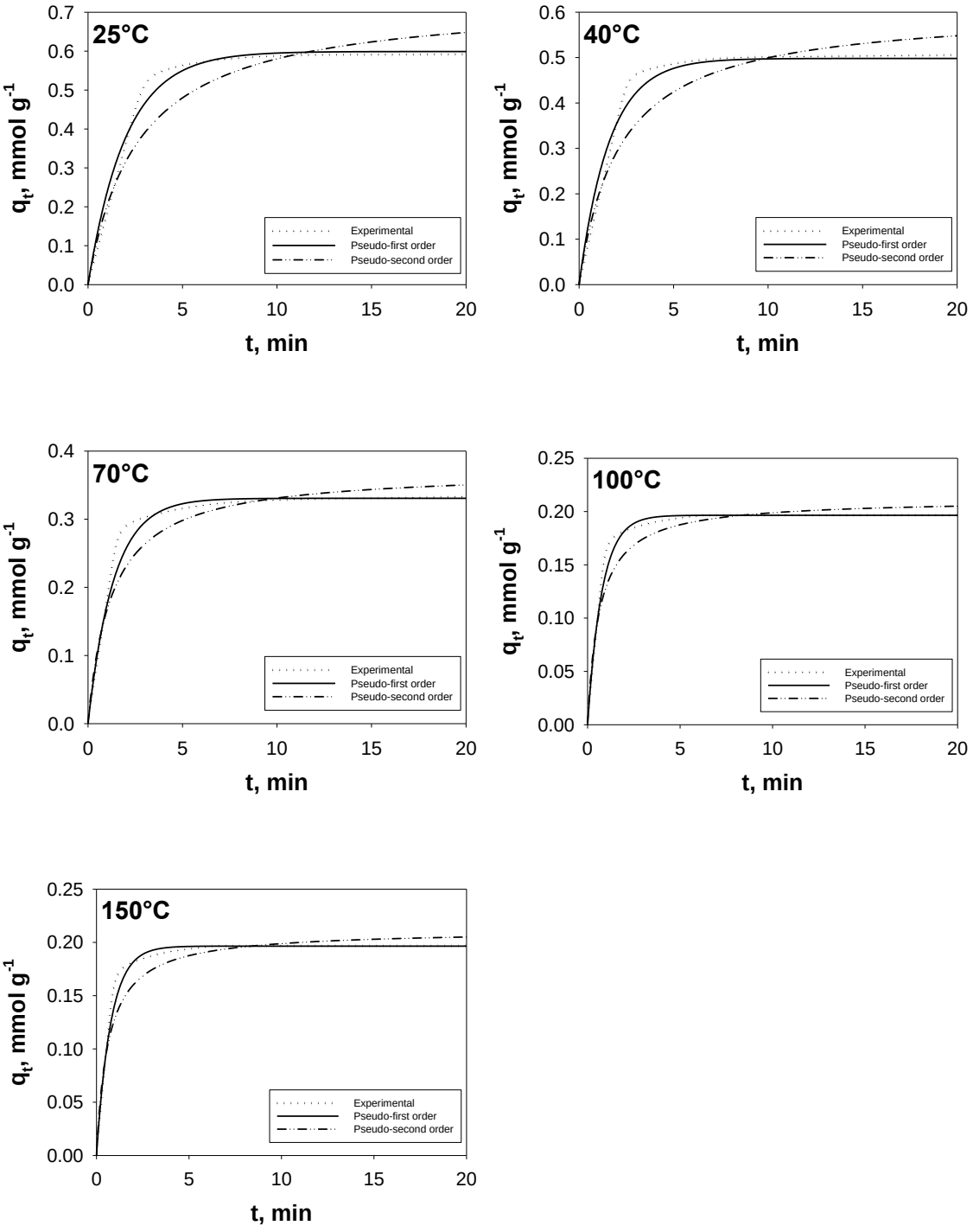

Fig. 11. Experimental (dotted line) CO_2 uptake on the natural tuff and corresponding fit to the pseudo-first (solid line) and pseudo-second (dashed line) order kinetic models at different adsorption temperatures.

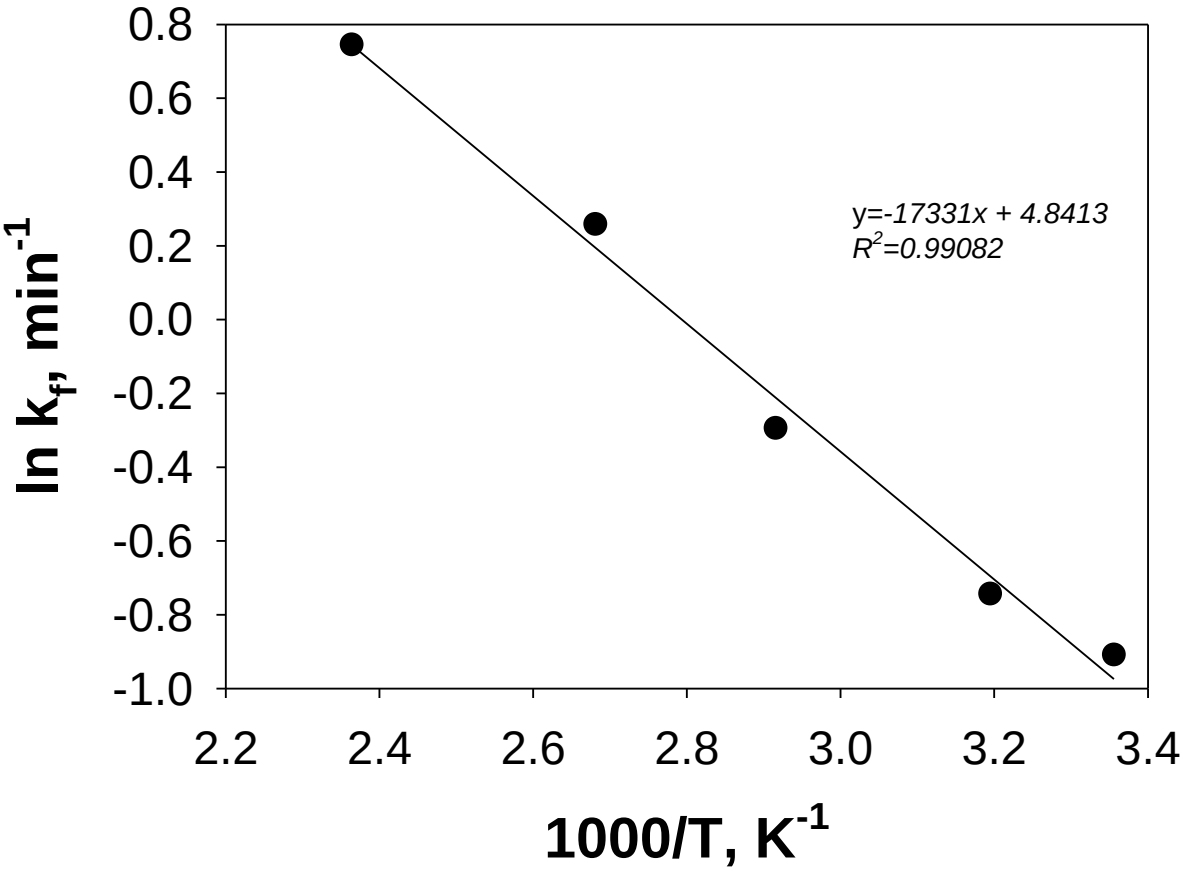

Fig. 12. Arrhenius plot: logarithm of the kinetic constant versus inverse of absolute temperature.

Table 1. Physical properties of the natural tuff.

Particle size, μm	400-600
Particle porosity, -	0.339[a]
Absolute density, g mL^{-1}	2.241[a]
Tap density, g mL^{-1}	0.810
Surface area, m^3 g^{-1}	141[b]
Specific heat, J g^{-1} K^{-1}	1.3
Minimum fluidization velocity, m s^{-1}	0.168

[a] MIP; [b] ref. [23]

Table 2. Results of CO_2 adsorption tests on the natural tuff.

%CO_2 %vol.	25°C				40°C				70°C				100°C				150°C			
	q_e mmol g^{-1}	t_b s	$\Delta\tau$ s	ψ %	q_e mmol g^{-1}	t_b s	$\Delta\tau$ s	ψ %	q_e mmol g^{-1}	t_b s	$\Delta\tau$ s	ψ %	q_e mmol g^{-1}	t_b s	$\Delta\tau$ s	ψ %	q_e mmol g^{-1}	t_b s	$\Delta\tau$ s	ψ %
1	0.216	332	225	51.972	0.164	280	160	59.170	0.089	183	92	68.373	0.047	66	69	71.255	0.028	40	42	72.570
3	0.347	222	110	67.149	0.265	201	83	69.371	0.166	131	36	71.499	0.077	47	27	73.461	0.046	27	25	75.471
5	0.426	190	76	70.472	0.348	165	52	73.352	0.196	84	32	75.786	0.111	44	24	76.281	0.067	26	23	77.446
10	0.561	144	43	72.999	0.491	128	31	75.617	0.331	76	23	76.912	0.200	41	19	77.302	0.124	24	17	78.696
15	0.643	111	29	74.513	0.593	106	24	76.627	0.404	68	18	77.400	0.256	39	17	78.222	0.167	23	15	79.393
20	0.710	104	23	76.889	0.659	94.998	21	78.187	0.453	64	17	78.995	0.306	37	16	79.606	0.198	21	14	80.479

Table 3. Langmuir and Freundlich adsorption equation parameters and fitting comparison.

T, °C	Langmuir				Freundlich				
	q_L mmol g^{-1}	K_L atm^{-1}	R^2 -	*HYBRID* %	k_F mmol g^{-1} $atm^{-1/n}$	n -	$1/n$ -	R^2 -	*HYBRID* %
25	0.826	24.988	0.994	0.526	1.341	2.616	0.382	0.999	0.035
40	0.859	14.968	0.994	0.479	1.430	2.129	0.469	0.999	0.020
70	0.684	9.526	0.994	0.352	1.128	1.808	0.553	0.999	0.076
100	0.636	4.556	0.997	0.212	0.939	1.448	0.690	0.999	0.072
150	0.493	3.373	0.998	0.129	0.665	1.347	0.742	0.999	0.055

Table 4. Thermodynamic properties for CO_2 adsorption on the natural tuff.

ΔH^0 kJ mol^{-1}	ΔS^0 kJ mol^{-1}	ΔG^0 kJ mol^{-1}				
		18°C	*40°C*	*70°C*	*100°C*	*150°C*
-17.04	-0.031	-7.709	-7.239	-6.300	-5.360	-3.794

Table 5. Values of the pseudo-first order and pseudo-second kinetic model parameters and fitting comparison.

T, °C	Pseudo-first order				Pseudo-second order			
	q_e mmol g^{-1}	k_f min^{-1}	R^2 -	*HYBRID* %	q_e mmol g^{-1}	k_s g $mmol^{-1}$ min^{-1}	R^2 -	*HYBRID* %
25	0.605	0.403	0.995	0.0672	0.734	0.516	0.987	0.111
40	0.513	0.476	0.997	0.0636	0.607	0.766	0.988	0.109
70	0.331	0.745	0.998	0.0432	0.372	2.173	0.989	0.084
100	0.197	1.295	0.999	0.0294	0.212	7.372	0.995	0.067
130	0.122	2.108	0.999	0.0244	0.129	21.052	0.996	0.047

Table 6. Sorbent rate and energy penalties for CO_2 capture.

		1	**2**	**3**	**4**
	T uptake, °C	25	40	70	25
	q_e, *mol* kg^{-1}	0.643	0.593	0.404	1.286
a) TS - 105 °C					
Sorbent rate	kg s^{-1}	5.967	6.586	10.835	2.702
Penalty H_t	MJ_t kg^{-1}	6.311	5.700	5.093	3.069
Penalty W_e	MJ_e/kg	0.000	0.000	0.000	0.000
b) VS - 0.05 atm					
Sorbent rate	kg s^{-1}	14.630	12.958	15.263	3.691
Penalty H_t	MJ_t kg^{-1}	0.041	0.041	0.041	0.041
Penalty W_e	MJ_e kg^{-1}	-0.288	-0.302	-0.331	-0.288
c) TS & VS - 70 °C & 0.10 atm					
Sorbent rate	kg s^{-1}	10.175	12.117	43.488	3.324
Penalty H_t	MJ_t kg^{-1}	6.069	4.898	0.387	2.244
Penalty W_e	MJ_e kg^{-1}	-0.249	-0.241	-0.223	-0.249

***Declaration of Interest Statement**

The Authors, whose names are listed immediately below, certify that:

- they have NO affiliations with or involvement in any organization or entity with any financial interest, or non-financial interest in the subject matter or materials discussed in this manuscript
- no funding was received for this work

Paola Ammendola

Federica Raganati

Riccardo Chirone

Francesco Miccio